



Contents lists available at ScienceDirect

Global and Planetary Change

journal homepage: www.elsevier.com/locate/gloplacha

The role of land surface processes on the mesoscale simulation of the July 26, 2005 heavy rain event over Mumbai, India

Hsin-I Chang^a, Anil Kumar^{a,b}, Dev Niyogi^{a,*}, U.C. Mohanty^c, Fei Chen^b, Jimy Dudhia^b

^a Purdue University, West Lafayette, IN, USA

^b National Center for Atmospheric Research, Boulder, CO, USA

^c Indian Institute of Technology, Delhi, New Delhi, India

ARTICLE INFO

Article history:

Accepted 8 February 2008

Available online xxx

Keywords:

Heavy rain

Mumbai

Mesoscale convection

Weather research and forecast model

Indian summer monsoon

Land surface processes

ABSTRACT

A record-breaking heavy rain event occurred over Mumbai, India on July 26th, 2005 with 24-h rainfall exceeding 944 mm. Operational weather forecast models failed to predict the intensity and amount of heavy rainfall. The objective of this study was to test the impact of the three different land surface models when coupled to the Weather Research Forecasting (WRF), and also to investigate the ability of the WRF model to simulate the Mumbai heavy rain event. Numerical experiments were designed using the WRF model, with three nested domains (30, 10, and 3.3 km grid spacing). Results confirmed that the simulated rainfall is sensitive to the grid spacing (with finer grids leading to higher rainfall). Results also suggest that simulated precipitation amounts are sensitive to the choice of cumulus parameterization (with Grell–Devenyi cumulus scheme performing relatively best). To reduce the confounding impact of cumulus parameterization in studying the impacts of land surface models, we evaluated results for the 3.3 km grid spacing domain with explicit convection. Simulations were performed from 12Z, July 25th to 00Z, July 27th with identical boundary conditions and model configurations for three different land surface models (the Slab, the Noah, and a modified version with photosynthesis module—the Noah-GEM). The model results were compared with observed rainfall, surface temperature, and operational soundings over three locations: Mumbai, Bangalore and Bhopal. Model results showed that: (i) The simulated rainfall was sensitive to the chosen land surface model. The rainfall spatial distributions, as well as their temporal characteristics, were different for each of the three WRF runs with different LSMs. (ii) In contrast to the findings over mid-latitudes, the relatively simpler Slab model had a relatively better performance than the modestly complex Noah and Noah-GEM LSMs. For example, the highest observed rainfall over Mumbai was 944 mm and the simulated amounts for Slab, Noah and Noah-GEM runs were 781 mm, 733 mm and 678 mm, respectively. (iii) Overall, the Slab model simulated a relatively cooler surface and a shallower boundary layer. Most significantly, the Slab model resulted in a convergence hotspot at both the 850 mb and 500 mb levels, which lead to high moisture accumulation and higher rainfall activity over Mumbai. Noah and Noah-GEM, on the other hand, resulted in a divergence zone over Mumbai and the Western Ghats leading to more widespread runs but relatively lower rainfall amounts over Mumbai. Additional synthetic experiments were performed to test the sensitivity of land use land cover, the model start time and run duration. Results indicated that the WRF model was able to reproduce several features of the Mumbai rain event, and that the land surface representations would have substantial impact on the heavy rain simulations. Future studies with more up to date land use land cover data, and regional calibration of the land surface model parameters, show the potential for improving the performance of the Noah-WRF over the Indian monsoon region.

© 2008 Elsevier B.V. All rights reserved.

1. Introduction

On July 26th, 2005, the Indian Meteorology Department (IMD) observatory at Santa Cruz (19.2°N, 72.53°E) in northern Mumbai

recorded 944 mm of rainfall over a 24 h period (ending 0300 UTC on July 27th, 2005), while the Colaba observatory (18.93°N, 72.85°E), (about 25 km south of Santa Cruz) recorded 74 mm for the same period. The highest rainfall recorded for the event was 1049 mm at Lake Vihar in northern Mumbai (19.14°N, 72.53°E), (Jenamani et al., 2006). The rain gauge observations for this rain event are shown in Fig. 1a. The previous record of the heaviest 24-h rainfall over Mumbai was 578 mm for Colaba in 1974, and 399 mm for Santa Cruz in 1991. The Tropical Rainfall Measuring Mission (TRMM) satellite, which

* Corresponding author. Department of Agronomy & Department of Earth and Atmospheric Sciences, Purdue University, West Lafayette, IN 47907, USA. Tel.: +1 765 494 6574.

E-mail address: dniyogi@purdue.edu (D. Niyogi).

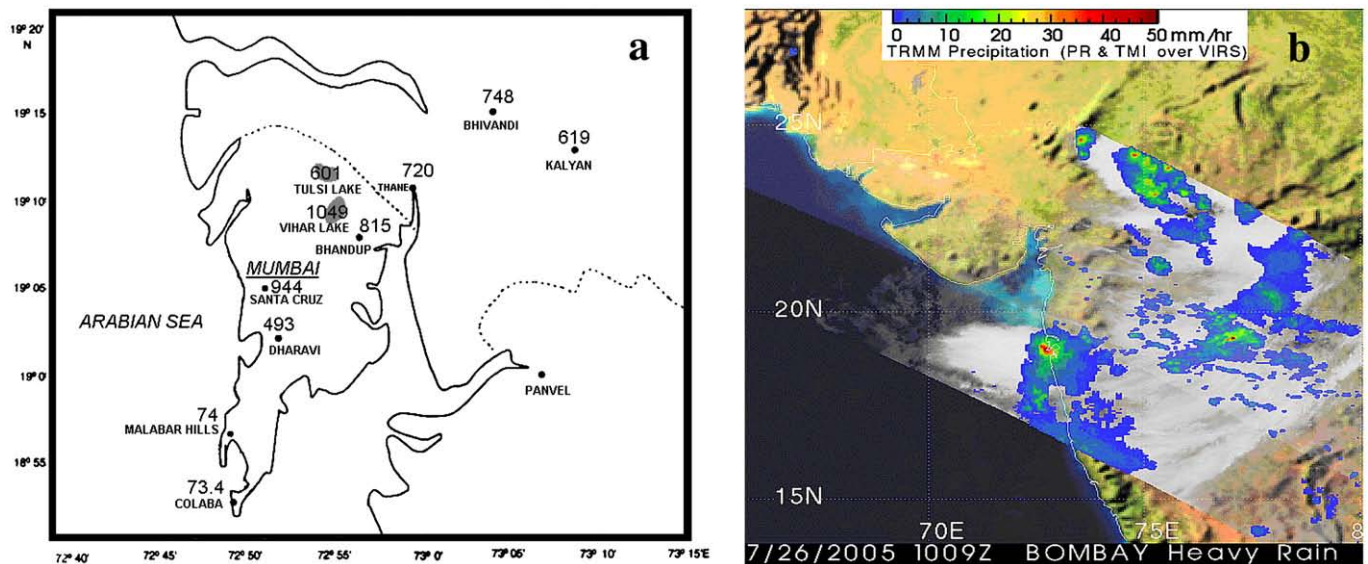


Fig. 1. (a) Rainfall observations across Mumbai (mm); (b) TRMM rainfall rate (mm/h) for July 25–27, 2005 (Source: NASA Goddard Space Flight Center/Tropical Rainfall Measurement Mission Extreme events archive. http://trmm.gsfc.nasa.gov/publications_dir/bombay_july05_rain.html).

passed over Mumbai at 3:39 PM local time (1009 UTC), also captured a highly localized and intense rainfall locale over the Indian sub-continent (Fig. 1b).

Jenamani et al. (2006) studied the observational and forecasting aspects of the Mumbai rain with satellite and surface observations. They also compared this rain event case with other historical intense rain episodes over India. Observations indicated that a weak monsoon condition existed between July 19th and 22nd. The monsoon strengthened due to a low pressure system over the northern area of the Bay of Bengal on July 23rd. Jenamani et al. (2006) concluded that the low pressure system positioned the rain bands over the

Western Ghats, and mesoscale interactions lead to the formation of the severe Mumbai rainfall. Shyamala and Bhadram (2006) extended the analysis using observational data for synoptic and thermodynamic fields and radar, and visible satellite imagery. They confirmed that a cloud band formed over the Arabian Sea on July 25th, which corresponded with strong low level winds over Mumbai with mid-tropospheric dryness, which may have contributed to the heavy rain.

Per many media reports, the event was not correctly forecasted by the operational weather forecast centers. The heavy deluge thus caught the public by surprise and led to loss of over 3.5 billion USD and over thousand human beings (NCDC, 2007). To synthesize the

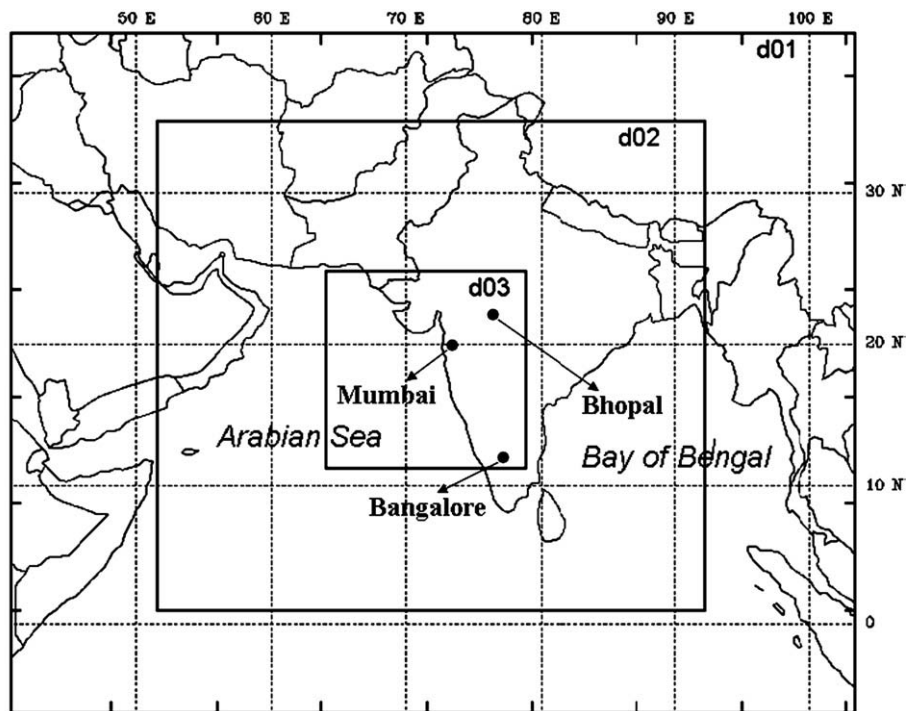


Fig. 2. Domains used for WRF simulations with 30 km (domain d01), 10 km (domain d02), and 3.3 km (domain d03) horizontal grid spacing and 31 vertical layers. Also, three selected meteorological stations for which sounding and surface data are available for comparisons within the model's third domain (d03) results are indicated. The three locations are Mumbai, Bangalore, and Bhopal.

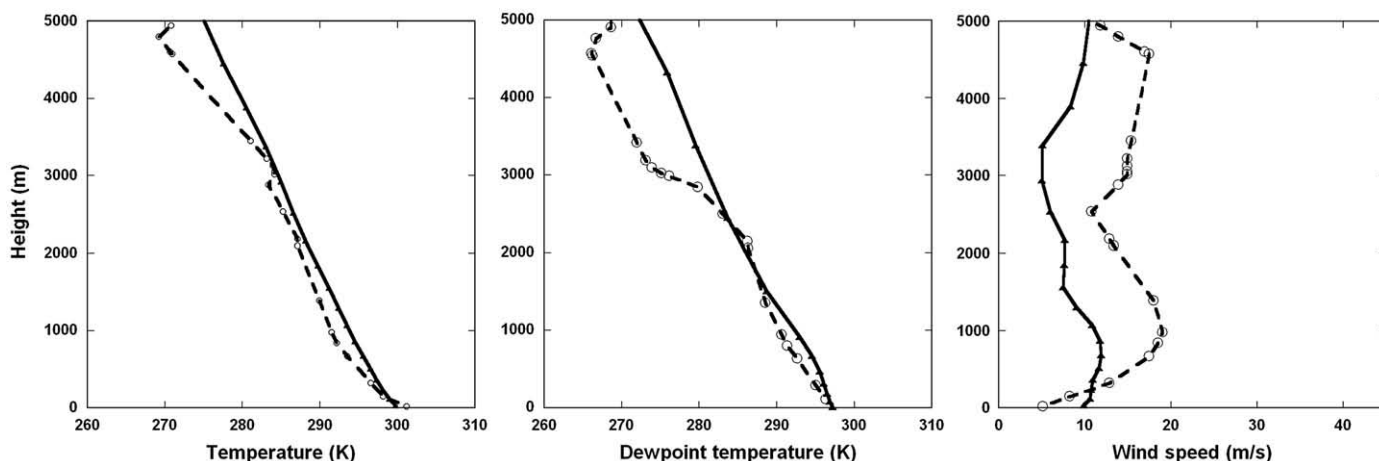


Fig. 3. Observed (dashed line with open circle) and WRF control (solid line with closed triangle) sounding data over Mumbai (19.14°N, 72.53°E) in temperature (K), dew point temperature (K), and wind speed (m s^{-1}) profiles valid 00Z, July 26th, 2005.

performance of the operational models, Bohra et al. (2006) reanalyzed the Mumbai rain event using five different operational numerical weather prediction (NWP) models. Experiments were also performed with two different initial and boundary conditions for the UK Meteorological Office (60 km grid spacing), and the Indian National Centre for Medium Range Weather Forecasting (NCMRWF) (150 km grid spacing). Although global forecasting systems are not expected to produce mesoscale forecasts, the NCMRWF global model simulated a weak hotspot (20 mm of rainfall) over Mumbai, and on 0300, UTC July

27 simulated the precipitation maxima of 40 mm of rain further south of Mumbai. The higher resolution model experiments (40 km resolution) from the European Centre for Medium-Range Forecasting (ECMWF) simulated between 40 and 100 mm of precipitation (well below the observed 944 mm rainfall amount). Results from retrospective analysis concluded that the performance with mesoscale models was relatively better: the accumulated rainfall amount came closer to the observations when using initial conditions in higher resolution.

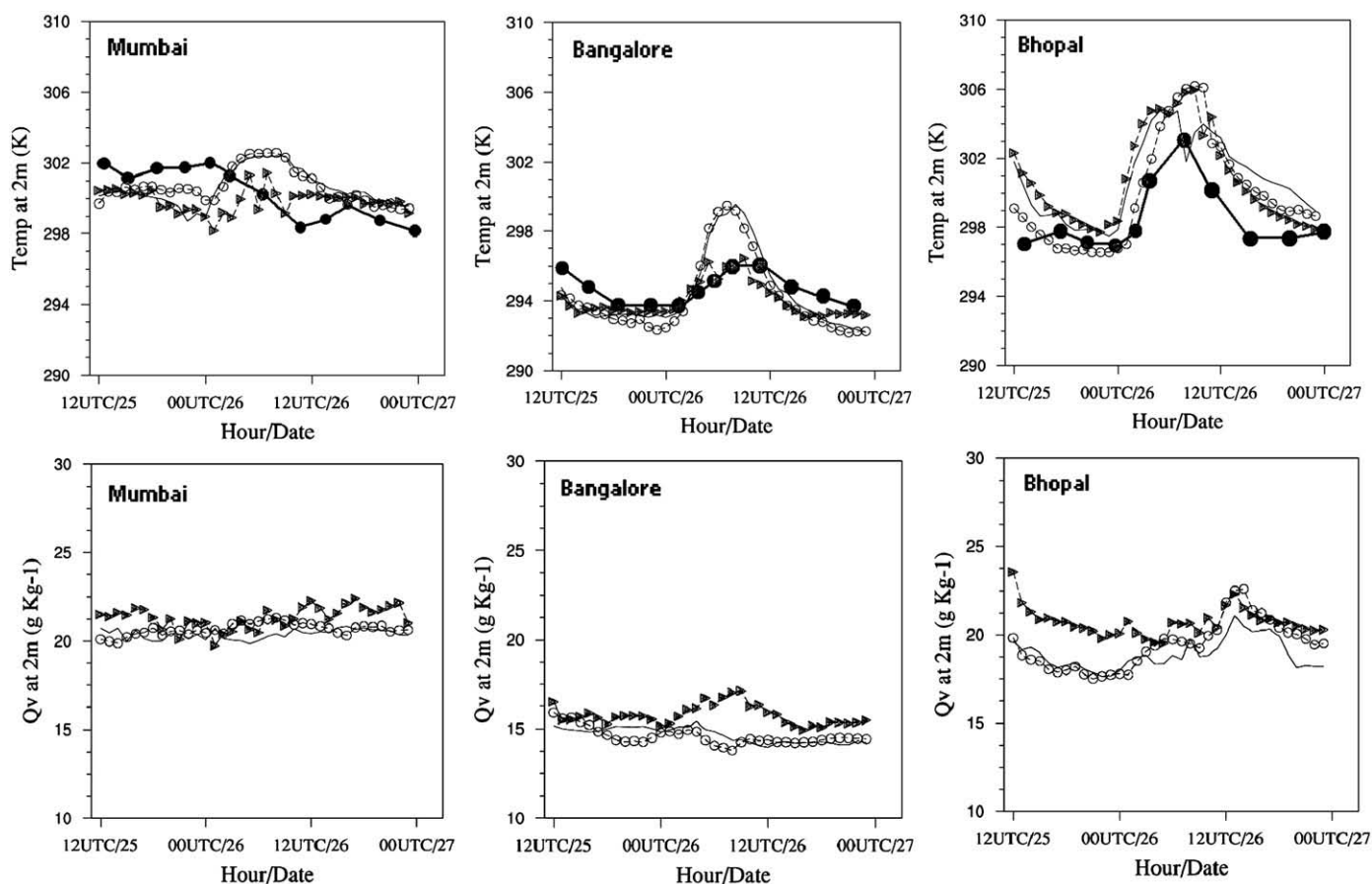


Fig. 4. Air temperature (K, first row) and surface humidity (g Kg^{-1} , second row) time series from observations (thick solid line with closed circle, when available) and LSM simulations (Noah—solid line, Slab—dashed line with closed triangle, Noah-GEM—dashed line with open circle).

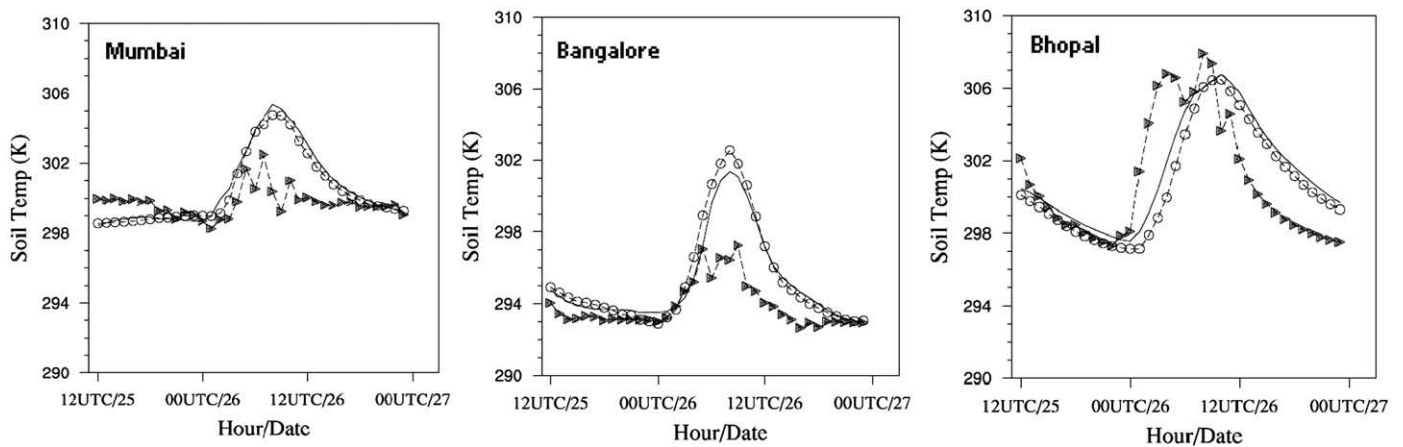


Fig. 5. Same as Fig. 4 but for soil temperature (K) time series plots.

Following Bohra et al. (2006), Vaidya and Kulkarni (2006) used a mesoscale model—the ARPS (Advanced Regional Prediction System)—to simulate this event. They adopted a 40 km grid spacing and conducted a series of experiments with model domain size and later boundary conditions. They concluded that the heavy rain episode (381 mm) from 09Z–12Z on July 26th might have been due to a cloudburst phenomenon, and the continuous rainfall (563 mm) between 12Z, July 26th and 03Z, July 27th could have been caused by the continuous regeneration of thunderstorm activity under the influence of mesoscale cloud complexes.

2. Study objectives

Building on the past studies of heavy rain events over India, and the July 26th Mumbai rain in particular, we know that mesoscale model results are sensitive to the grid spacing (finer grid spacing leading to higher rainfall amounts), and cumulus parameterizations (Venkata Ratnam and Cox, 2006). Further, while it is known that land atmosphere interactions affect mesoscale processes, the impact of land surface processes on the simulation of the Mumbai rain event is unknown. The WRF is gaining popularity with various weather research and

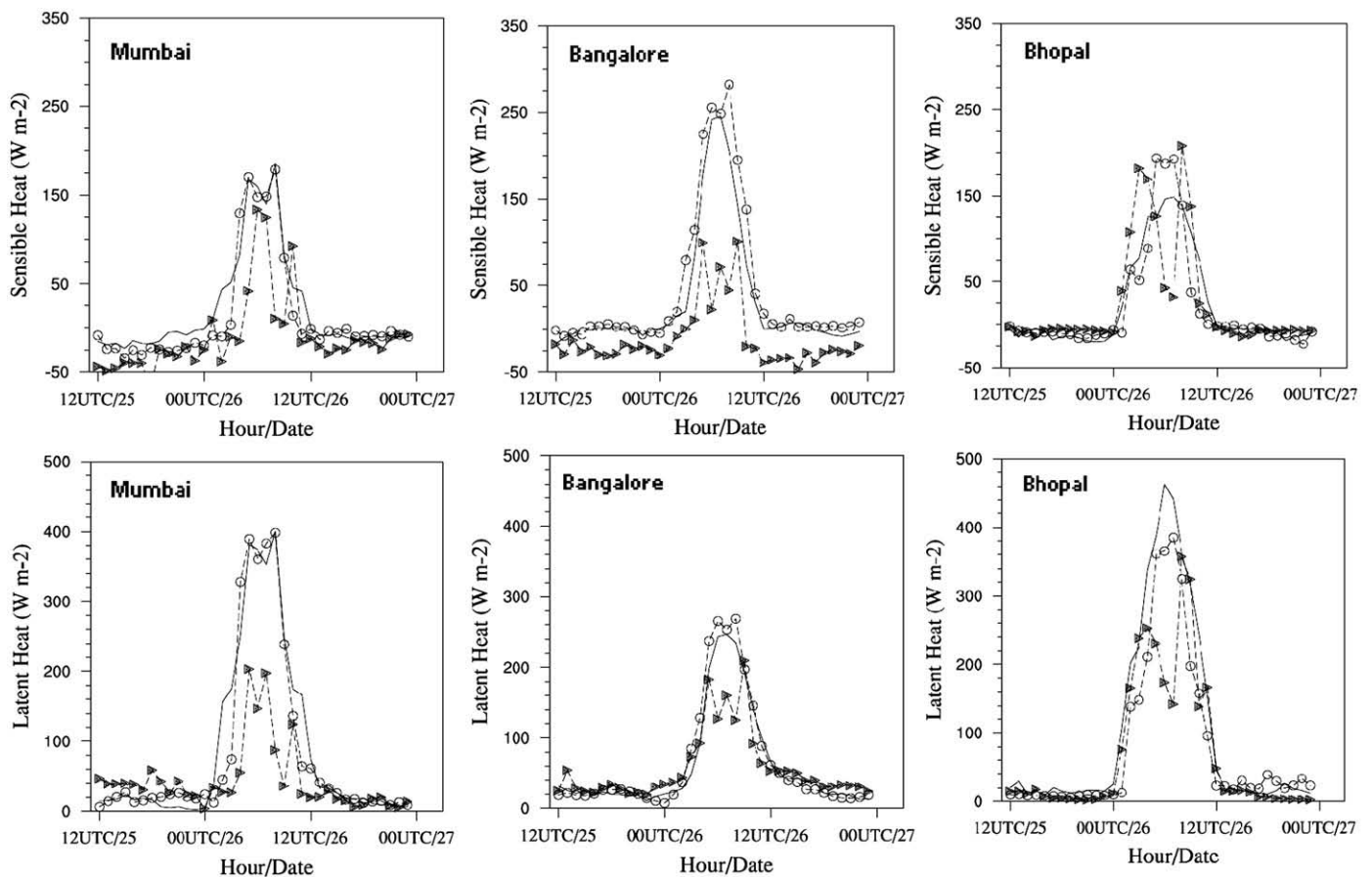


Fig. 6. LSM results for the same locations as in Fig. 5 for sensible heat flux (W m^{-2} , first row) and latent heat flux (W m^{-2} , second row) (Noah—solid line, Slab—dashed line with closed triangle, Noah-GEM—dashed line with open circle).

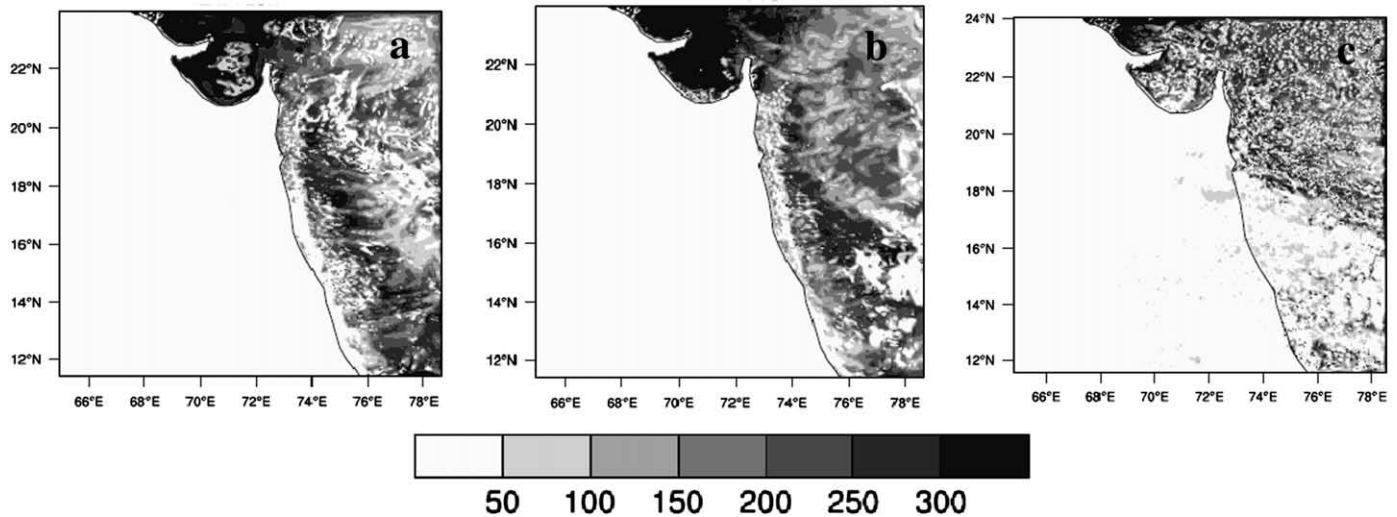


Fig. 7. Sensible heat flux (W m^{-1}) for (a) WRF control run (Noah LSM), (b) Noah-GEM, and (c) Slab at 00Z, July 26th, 2005 at 09Z, July 26th, 2005.

operational groups, therefore the relevance of the scope of testing the ability of WRF to simulate the Mumbai heavy rain is broad. In addition, the Indian region has also been identified as a land-atmosphere coupling hotspot in the multi-model Global Land-Atmosphere Coupling Experiment (Koster et al., 2004). Thus, the sensitivity experiments in this paper offer further information on the impact of land surface processes on coupled land-atmosphere models over India. Therefore, the objective of this study is to test the impact of different

land surface models coupled to the Weather Research Forecasting model (WRF). A related objective is to investigate the ability of the WRF model to simulate the heavy rain event that occurred over Mumbai on July 26th, 2005. The study also builds on the recent results of Trier et al. (2004), Holt et al. (2006), Niyogi et al. (2006) and Yasunari et al. (2006) which suggest that detailed land surface models can enhance model performance in predicting mesoscale convection and precipitation forecast.

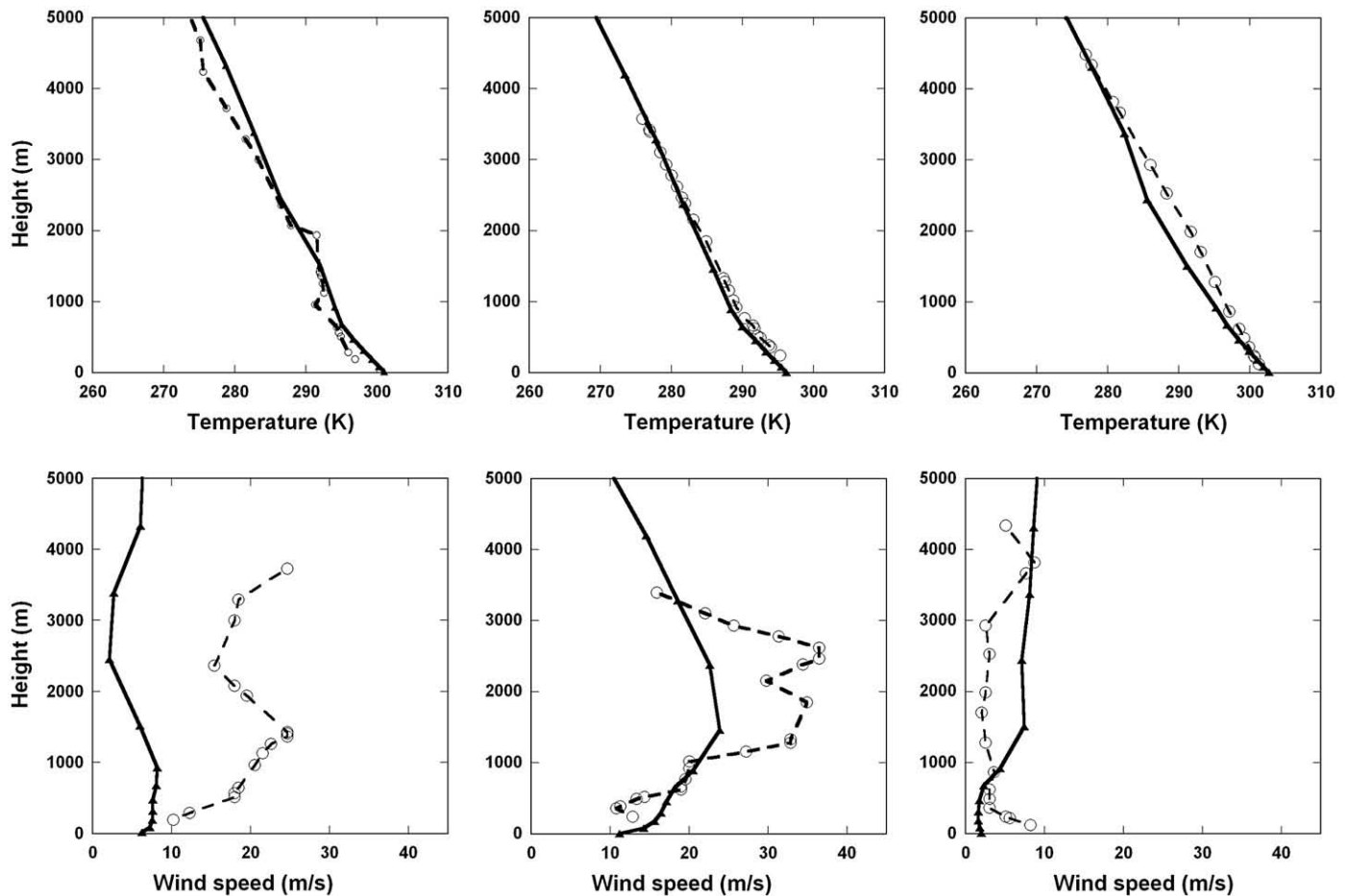


Fig. 8. Vertical profile from observed (dashed line with open circle) and model control run (solid line with closed triangle) at 12Z, July 26th, 2005 for temperature (first row) and wind speed (second row) profile up to 5 km at Mumbai (first column), Bangalore (second column), and Bhopal (third column).

The following section discusses the Mumbai rain event in relationship to the WRF set up and the experiment design. The results from the land surface model sensitivity experiments are shown in Section 4. Study conclusions are summarized in Section 5.

3. Model configuration and experimental set up

Numerical experiments are conducted with the WRF model Advanced Research Version. The WRF is a non-hydrostatic, primitive-equation model. We configured the WRF model with three one-way nested domains with grid spacings of 30, 10 and 3.3 km centered over Mumbai (19.12°N, 72.85°E) (Fig. 2). The outermost domain covered the Arabian Sea, the Indian sub-continent, and the Bay of Bengal, as well as parts of Africa to fully capture synoptic feedbacks. Domain 2 covers the Asian monsoon region including the Himalayas, the Indian sub-continent, and the Arabian Sea to capture the regional flow patterns. This design also captures the evolution of a low pressure system off the Bay of Bengal that was seen in the observation. The innermost domain (domain 3) covers part of the west coast of India in order to focus on the heavy rain locale. To capture the rain event, the simulation period was set from 12Z, July 25th to 00Z, July 28th. The model was configured with 31 vertical levels (1013 mb to 50 mb). Surface properties such as vegetation/land use data were prescribed by the 24 unique United States Geological Survey (USGS) land use categories with different surface albedo, moisture, emissivity, and roughness length values assigned to each category; topography was prescribed according to USGS terrain data. Also shown in Fig. 2 are the locations of the three selected weather stations with available surface and upper air observation data.

Vaidya and Kulkarni (2006) conducted experiments with domain size and lateral boundary condition for this event. Following their conclusions, the initial lateral and surface boundary conditions were prescribed based on 1°×1° National Center for Environmental Prediction (NCEP) reanalysis data. Observation indicated a strengthening monsoon pattern and an off-shore low pressure system over the Arabian Sea and the Bay of Bengal (figure not shown). The NCEP reanalysis data shows the low pressure system over the Bay of Bengal (around 20°N), but the off-shore low over the Arabian Sea is not represented well, which can introduce uncertainty in the model results. The errors in the initial conditions used in WRF model may led to the inaccuracy of the simulation results. We conducted two test runs with different start times (06Z and 18Z instead of 12Z, not shown) and confirmed that this error in the NCEP reanalysis is not dominant.

The WRF model has options for different physical parameterizations such as the boundary layer, convection, and radiation schemes. We also conducted tests with the Kain–Fritsch (KF), Betts–Miller–Janjic (BMJ), and Grell–Devenyi (GD) convective schemes. Our tests confirmed that the model results are particularly sensitive to the choice of convective parameterizations (Venkata Ratnam and Cox, 2006; Vaidya, 2006). In the case of this experiment, the Grell–Devenyi scheme showed the best model performance. To reduce dependence on cumulus parameterization, we focused on the high resolution (3.3 km) runs which had explicit convection. We tested several model settings (Chang et al., 2005) and selected a configuration with the MRF planetary boundary layer (PBL) scheme, the Dudhia shortwave radiation scheme, and the Goddard longwave radiation scheme with the Grell–Devenyi ensemble convective parameterization (CP) scheme as the control simulation. The choice of the control configuration was

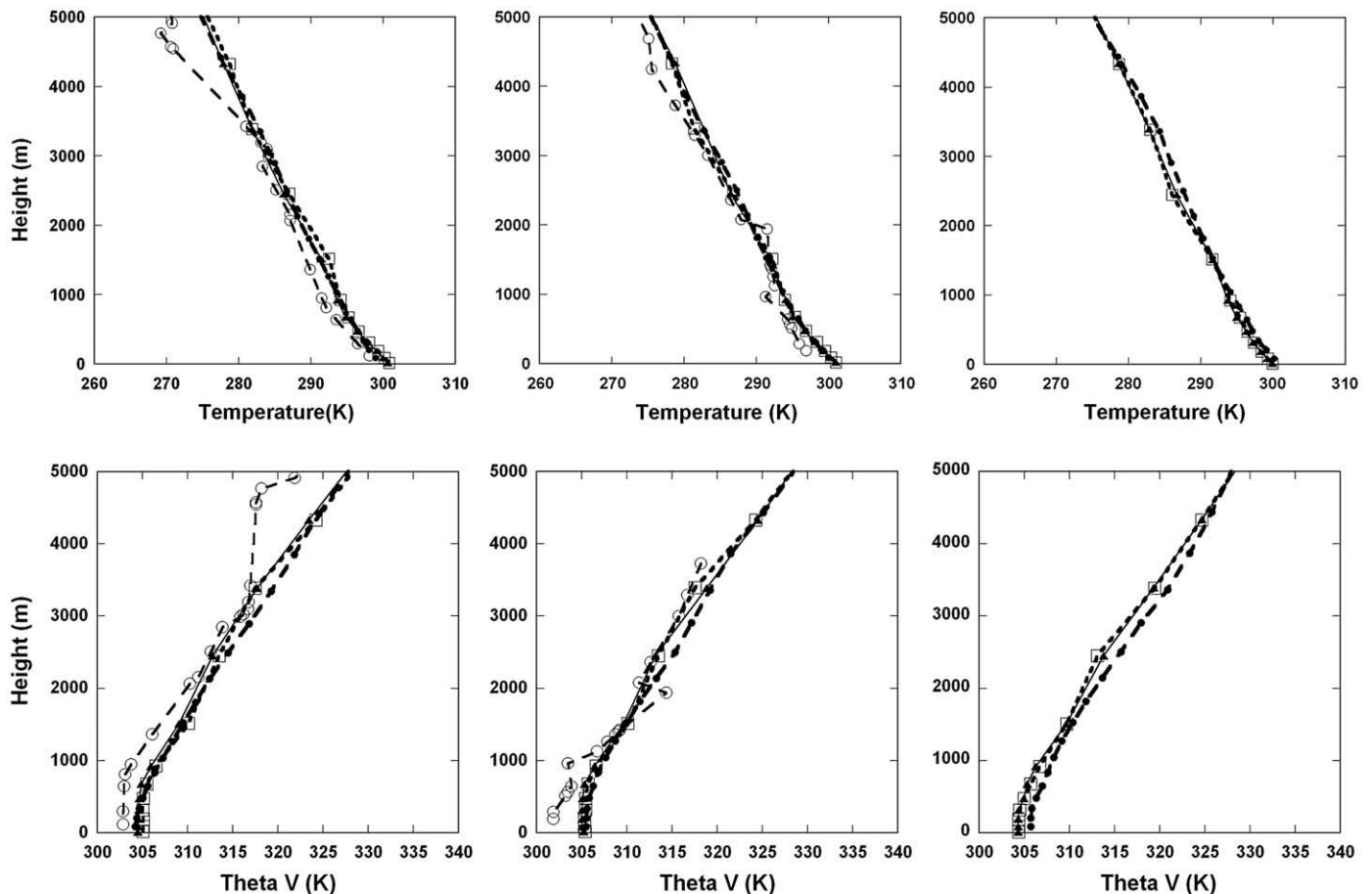


Fig. 9. Mumbai observed and simulated temperature (K) and Theta V (Virtual potential temperature, K) profiles for 00Z, July 26th (first column), 12Z, July 26th (second column) and 00Z, July 27th, 2005 (third column) (Observed—dashed line with open circle, Noah—solid line with closed triangle, Slab—dashed line with closed circle, Noah-GEM—dashed line with open square).

also guided by some recent high resolution model simulations over the Indian region (Azadi et al., 2002; Xavier et al., 2006).

The control simulation was conducted with the Noah LSM (Ek et al., 2003), which includes multi-layer soil with a single layer canopy. Typically, four soil layers (0.1, 0.3, 0.6 and 1.0 m thickness, with 2 m total soil depth) are prescribed for the description of the soil moisture/temperature feedback. The Noah LSM also contains a simple canopy resistance scheme (Chen and Dudhia, 2001), frozen soil parameterization (Koren et al., 1999), Noah LSM prognostic soil moisture and soil temperature, and net radiation and surface heat fluxes. To test the effect of the land surface schemes, we replaced the Noah LSM with a simple ‘Slab’ model and a more detailed ‘Noah-GEM’ model. The Slab experiment replaced the Noah with a simplified Slab land surface model. The Slab model prognosticates soil temperature (Deardorff, 1978) and has constant soil moisture availability. The Noah-GEM (gas exchange evapotranspiration model) is a CO_2 /photosynthesis-based model coupled within Noah which adds more detailed photosynthesis and canopy resistance/transpiration processes to the Noah LSM (Niyogi, 2000; Niyogi et al., 2006; Holt et al., 2006). Canopy resistance and transpiration was calculated using the Ball–Berry stomatal resistance model; this model was linked to a Noilhan and Planton (1989)-type prognostic soil moisture–soil temperature (SMST) scheme that simplified the representation for the mesoscale model applications. The WRF model configurations were identical except for the land surface model in the three experimental runs.

4. Results and discussions

In this section, the results for the Noah (control), Slab, and Noah-GEM runs will be presented. The model results are first

discussed for the diurnal variations. The variations in the surface parameters, vertical profiles, and mesoscale patterns of convergence/divergence as well as the circulation fields are analyzed. The resulting impacts on the model-simulated rainfall simulations are then discussed.

The study region has relatively few observing stations. Model results are compared with the observations (when available). We will focus on the model variability and timing of the three LSM runs. The three stations selected with available observation data were: Mumbai (coastal area, where highest precipitation occurred, 19.12°N, 72.85°E), Bangalore (southeast of Mumbai, 12.97°N, 77.58°E) and Bhopal (northeast of Mumbai, further inland, 23.28°N, 77.35°E). Bangalore and Bhopal provided contrasting locations for testing the model performance.

Fig. 3 shows the observed and the WRF control run simulated temperature, dew point temperature, and wind speed profiles for Mumbai at 00Z, July 26th. Observed sounding data over Mumbai (19.12°N, 72.85°E) indicate a low level jet with winds around 35 knots (18 m s^{-1}) between 925 and 850 mb. Above 500 mb, the atmosphere is dry with low relative humidity values. The Santa Cruz radiosonde observations indicate strong westerly winds (48–52 knots) in the lower atmosphere (figure not shown). The westerly winds provide favorable lower tropospheric conditions for moisture transport from the Arabian Sea.

The control run had a relatively better performance for temperature and a dew point temperature below the 3000 m level, and generally under-predicted the winds (Fig. 3). However, as discussed below, this performance varies over different locations in the study domain. The Skew-T analysis for the 00Z sounding (figure not shown) also indicated a large CAPE (Convective Available Potential Energy) of

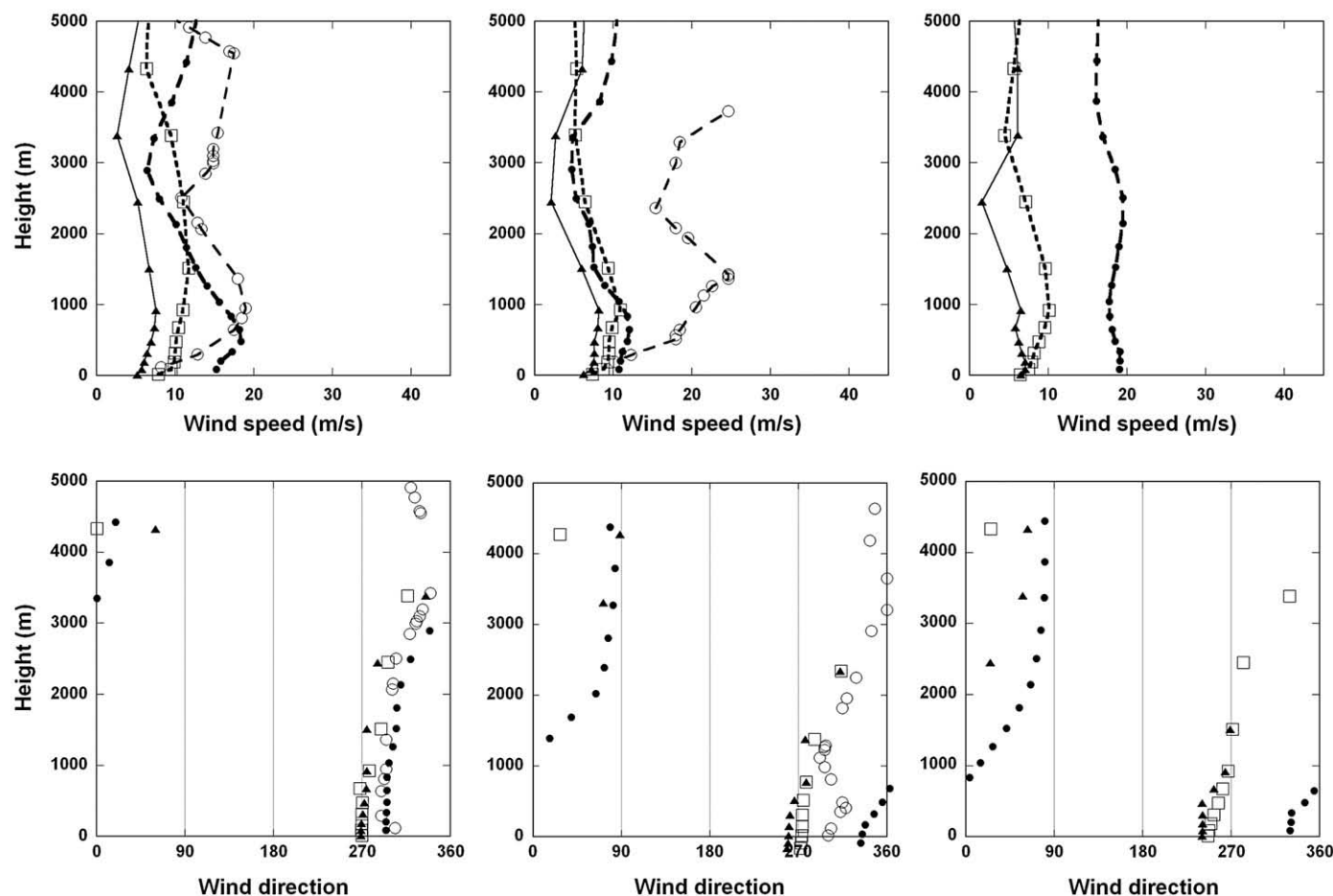


Fig. 10. Same as Fig. 9, but for wind speed (m s^{-1}) and wind direction vertical profiles (Observed—open circle, Noah—closed triangle, Slab—closed circle, Noah-GEM—open square).

3082 J kg⁻¹, a K-index of 29.1, and a near zero CIN (Convective Inhibition) indicative of a very unstable atmosphere. The simulated 00Z sounding (figure not shown) indicates a nearly saturated atmosphere between 500 and 700 mb and relatively drier air, yet with a high moisture content from 700 mb to the surface; also, only a small amount of CAPE (135 J kg⁻¹) and CIN (-17 J kg⁻¹) was simulated.

4.1. Temperature and humidity time series

Fig. 4 shows the time series plots for observed and model-simulated temperature and specific humidity over Mumbai, Bangalore, and Bhopal. Over Mumbai, the three runs produced a daytime peak and show significant scatter due to cloudiness and rain. Overall, the models simulated approximately 300 K during the morning and 303 K during the daytime, with the Slab model showing a larger hour-to-hour variability. The observations indicated a warm morning and an uncharacteristically rapid daytime cooling. This daytime cooling could be due to either the heavy rain or the spurious data and therefore cannot be verified. Over Bangalore, the temporal evolution is much more consistent between the LSM runs and the observations. The model runs generally have an exaggerated diurnal variation compared to the observation. Interestingly, the temperature variation from the simplest of the three LSMs (Slab) is closest to the observation. The Noah and Noah-GEM closely follow each other and simulate higher mid-day air temperature. Over the inland station at Bhopal, the three runs have a generally similar diurnal evolution, with the Noah-GEM best-resembling the observations. However, all the models over-estimated the maximum temperature over Bhopal by about 3 K.

Overall, with regards to air temperature simulation, all three LSM runs show differences, but with a consistent daytime over-prediction by about 3 K. The Noah and Noah-GEM runs usually had similar results, while the Slab showed different variations.

The simulated surface humidity showed less diurnal variation than air temperature. Over Mumbai, the three runs simulated surface humidity values between 20 and 22 g kg⁻¹, with the Slab being highest at night and the Noah being lowest throughout. Similar results were seen over Bangalore and Bhopal with the Slab run being about 2 g kg⁻¹ higher than the Noah and Noah-GEM runs. Typical values ranged ~14 to 16 g kg⁻¹ over Bangalore and 18 to 22 g kg⁻¹ over Bhopal.

The impact of the land surface models on the WRF simulated soil temperature is shown in Fig. 5. The Slab run generally resulted in lower (by 1 to 2 K) soil temperatures over Mumbai and Bangalore, and about 1 to 2 K warmer temperatures over Bhopal.

Each of the land surface models uses the same soil type, vegetation/land use datasets. So the main reason for these differences in soil and air temperatures can be attributed to the soil and air temperature computations in the LSMs. The diffusion equation used in the Slab is:

$$\frac{\partial T_s}{\partial t} = -\frac{1}{\rho_s C_s} d \frac{\partial F}{\partial Z}$$

T_s is the soil temperature (K), ρ_s is the density (kg m⁻³), C_s is the heat capacity (J kg⁻¹ K⁻¹), and F is the heat flux (W m⁻²). No vegetation processes are explicitly represented in the Slab model. A

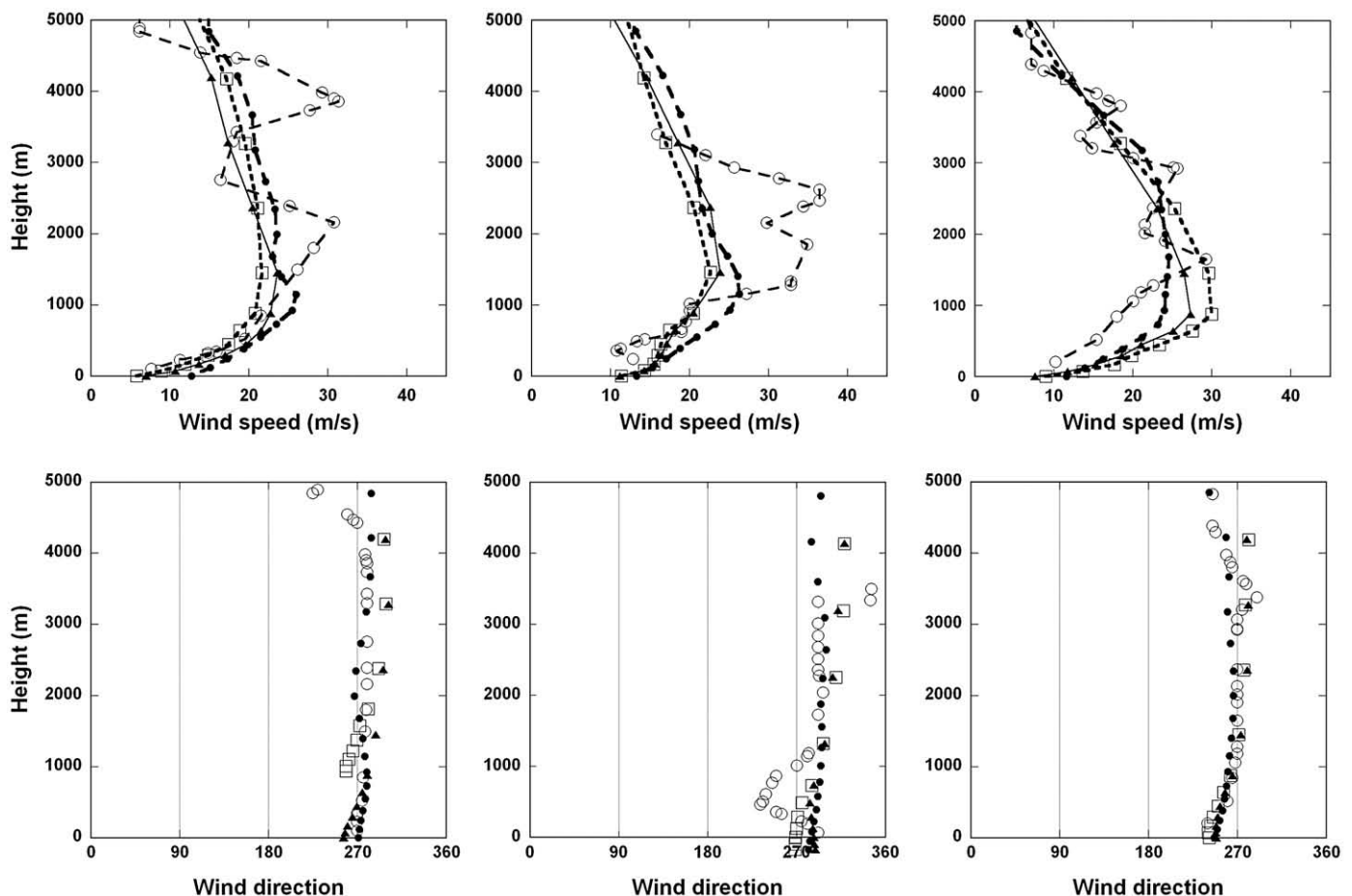


Fig. 11. Same as Fig. 10, but for wind speed (m s⁻¹) and wind direction vertical profiles for Bangalore.

different diffusion equation is used in the Noah and Noah-GEM models:

$$C(\theta) \frac{\partial T_s}{\partial t} = \frac{\partial}{\partial Z} \left[K_t(\theta) \frac{\partial T_s}{\partial Z} \right]$$

T_s is the soil temperature (K), C is the volumetric heat capacity ($\text{J m}^{-3} \text{K}^{-1}$), θ is the fraction of soil volume occupied by water, and K_t ($\text{W m}^{-1} \text{K}^{-1}$) is the thermal conductivity. The changes in soil temperature affect the air temperature via surface fluxes. In Noah, soil moisture impacts the heat capacity (C) and thermal conductivity estimates. Reviewing the over-prediction of the soil and air temperatures with Noah and Noah-GEM in this study, one possible factor for this error could be their known over-prediction of the thermal conductivity (K_t) under wet soil conditions (Chen and Dudhia, 2001).

As discussed in Niyogi et al. (2006), caution needs to be exercised in comparing grid values with point observation. Specific to the three selected points (Mumbai, Bangalore and Bhopal), the default values of the vegetation fractions (Mumbai: 0.12, Bangalore: 0.29, Bhopal: 0.17) are apparently lower than the observations. Overall, the three model runs lead to some broad similarities with the observations, while showing distinct differences between each other (particularly Slab).

4.2. Surface heat flux

The resulting impact of the different LSMs on the surface sensible heat flux (SHF) and latent heat flux (LHF) time series is shown in Fig. 6. Over Bangalore, Noah and Noah-GEM simulated about 200 W m^{-2} more than Slab. The SHF simulation results were similar over Mumbai

and Bhopal. Again, the SHF diurnal variability in Mumbai, Bangalore and Bhopal was consistent with the trend of air temperature and soil temperature variations. Noah and Noah-GEM simulated similar results for all three stations, while the Slab resulted in lower SHF over Mumbai and Bangalore. The LHF also showed a mid-day peak at all three stations. LHF values were high over Mumbai in the Noah and Noah-GEM, and generally comparable over Bangalore and Bhopal.

Fig. 7 shows the surface sensible heat flux variability from the three model runs valid 09Z, July 26th, 2005, which corresponds to the surface environmental conditions before the heavy rains. Noah and Noah-GEM exhibit relatively similar patterns, both in terms of the magnitude as well as the distribution. Regions around Mumbai and southern India show a region of large spatial gradient in surface fluxes. Satellite imagery indicates nearly overcast conditions (figure not shown), which reduces the magnitude of the fluxes. However, these gradients in surface fluxes can create mesoscale boundaries that provide pathways for moisture transport and regional convergence/divergence patterns, and is discussed in the following section. As compared to Slab, Noah and Noah-GEM runs simulated higher (and similar) LHF values (figure not shown). This would lead to a weaker convergence zone and more localized clouds in the Noah and Noah-GEM results and is discussed ahead.

4.3. Vertical profiles

The changes in the simulated surface thermodynamic features and surface energy fluxes also affected the vertical temperature and wind profiles within the model. In general, the WRF control run accurately simulated the air temperature profile for all three locations from surface

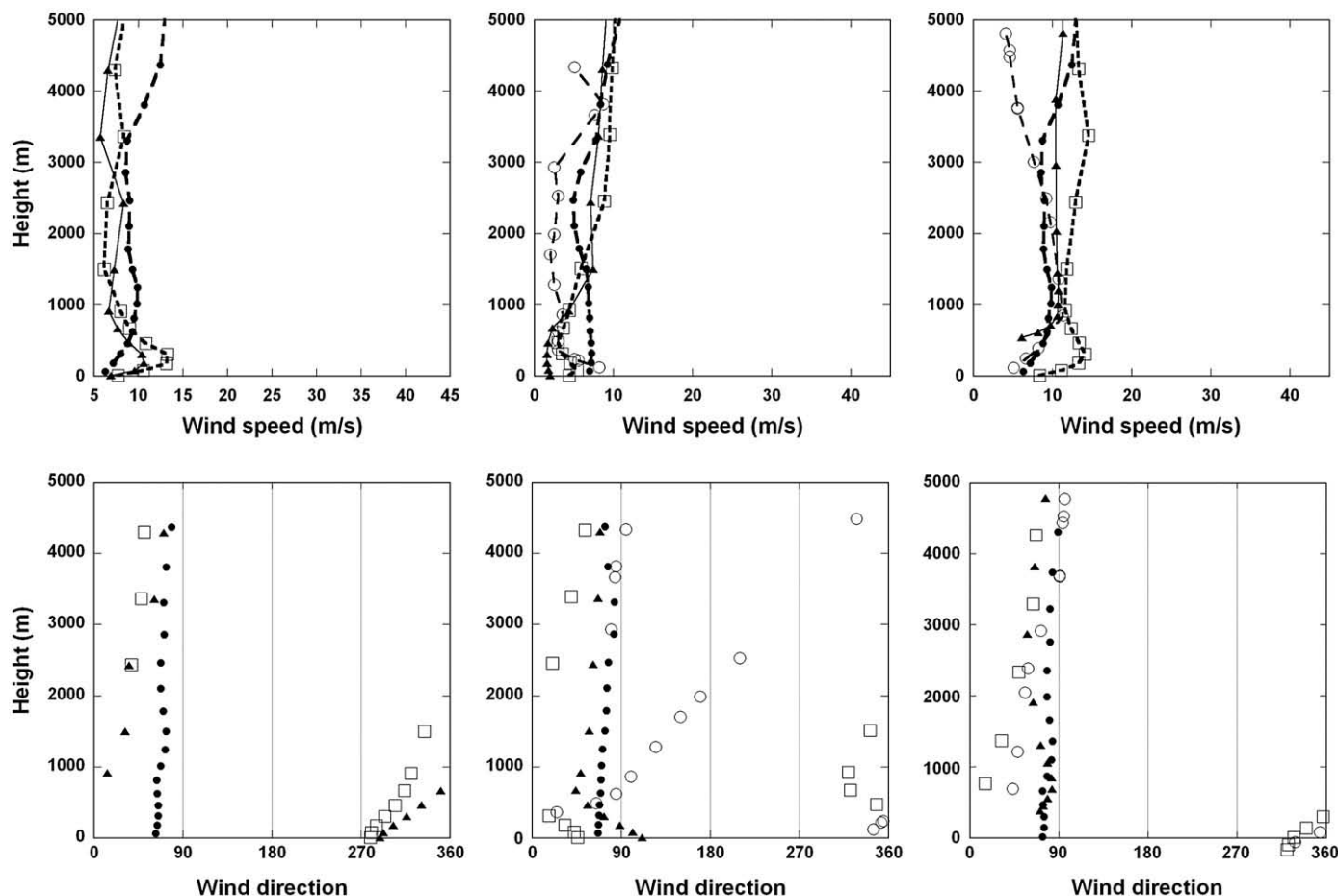


Fig. 12. Same as Fig. 10, but for wind speed (m s^{-1}) and wind direction vertical profiles for Bhopal.

to 5000 m (Fig. 8). However, the model performed relatively poorly in terms of simulating winds. Calmer winds were simulated over Mumbai. Over Bangalore, the WRF captured the higher wind speeds but missed the low level jet and its performance over Bhopal was modest.

Fig. 9 shows model-simulated air temperature and virtual potential temperature (θ_v), while Fig. 10 shows winds over Mumbai. We also estimated θ_e (equivalent potential temperature) in consideration of the high-moisture lands expected at the coastal locations. However, the values and variations were similar to θ_v and therefore not discussed here. Generally, the simulated θ_v values were 2 to 3 K higher than the observed. The observed θ_v and wind profile over Mumbai showed the internal boundary layer formation between 1000 and 3000 m, and a return circulation above 3000 m at 00Z (5:30 AM local time), July

26th. The three model runs generally simulated neutral boundary layers near the surface to 1000 m and a near stable lapse rate up to 3000 m. The three runs also correctly simulated near surface westerly winds around Mumbai between 00Z and 12Z July 26th, but had difficulty simulating the return circulation that was seen in the observations above 3000 m.

For Bangalore, the three LSM runs produced similar lapse rates with neutral condition below and stable upper air above the boundary layer. The θ_v values were about 1 to 3 K higher than observed (for 12Z, July 26th, figure not shown). Slab, Noah and Noah-GEM runs generally simulated similar winds (Fig. 11) with persistent westerly winds. Neither of the runs captured the upper air wind speed variations correctly, and simulated smoother wind speed profiles, and missing the westerly to

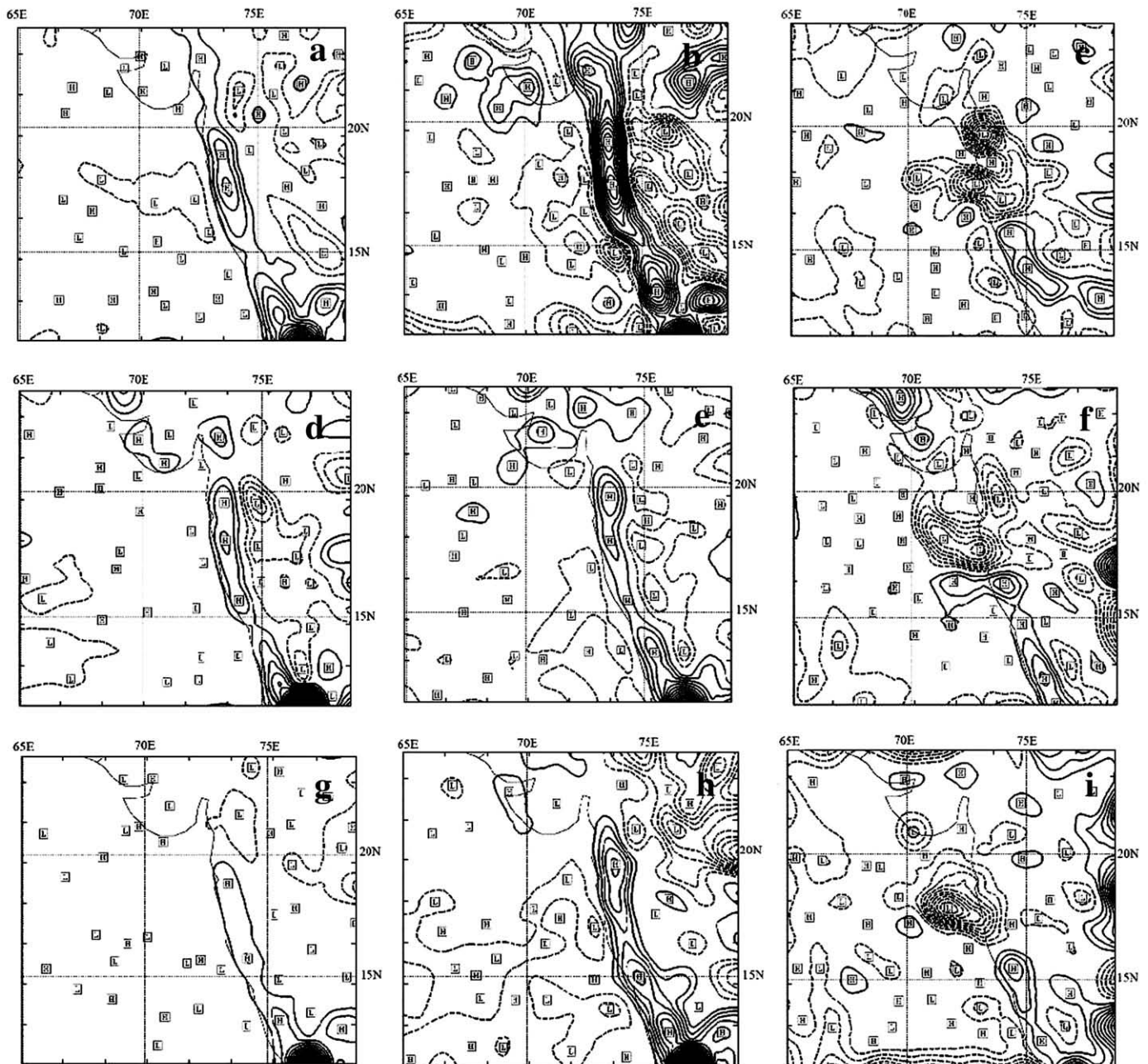


Fig. 13. Divergence/convergence plots at 850 mb level for WRF control run (Noah LSM, first column), Noah-GEM (second column), and Slab (third column). Plots are made in 12-h interval at 00Z, July 26th (first row), 12Z, July 26th (second row) and 00Z, July 27th (third row). Solid lines represent divergence with H, and dashed lines are for convergence activities with L.

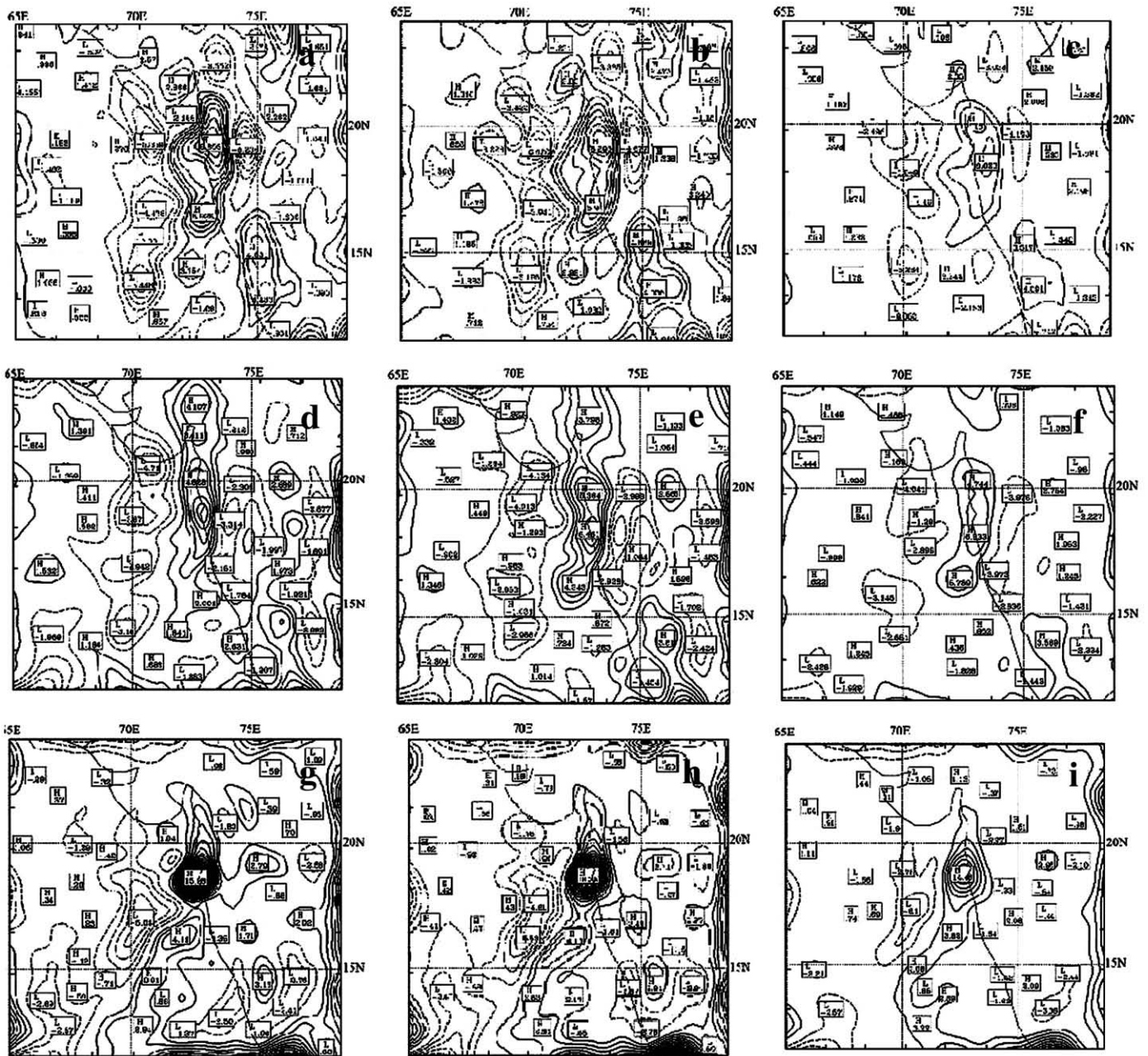


Fig. 14. Same as Fig. 13, but for 100 mb level.

south-westerly wind direction change at 12Z, July 26th. For the inland station (Bhopal), the model results show relatively better agreement with observations (Fig. 12).

4.4. Wind circulation and convergence/divergence

The difference in surface and boundary layer processes simulated by the three LSM runs also affect the regional circulation and convergence/divergence fields. The 850 mb winds in the second domain (not shown) indicated both the WRF control and the WRF Noah-GEM runs captured the low pressure system off the Bay of Bengal. In Noah-GEM, the low pressure system moved relatively faster with strong westerly winds and a further inland low pressure center. For the Slab model results, only strong wind shears were simulated, without any indication of low pressure circulation until 12Z, July 26th. In the Slab run, the low pressure

system off the Bay of Bengal did not move further westward until 00Z July 27th, mainly due to the newly formed low pressure center over Western India.

To further delineate the regional dynamical feedbacks associated with the three LSM runs, we computed the convergence/divergence fields at 850 mb, 500 mb and 100 mb. The divergence/convergence patterns show important differences between the three runs. Most notably, the Slab run produced a convergence hotspot over Mumbai; while in the Noah and Noah-GEM runs, the convergence zone is shifted more inland.

The Noah control run shows a divergence zone over Mumbai at 00Z, July 26th, which by 12Z forms a closed circulation cell over Mumbai in the 850 mb fields (Fig. 13). The cell weakened over the next 12 h, becoming weakly divergent at the 850 mb level. For the 500 mb (not shown) and 100 mb (Fig. 14) levels, results indicated a strongly divergent region above Mumbai at 00Z, July 26th with a convergence

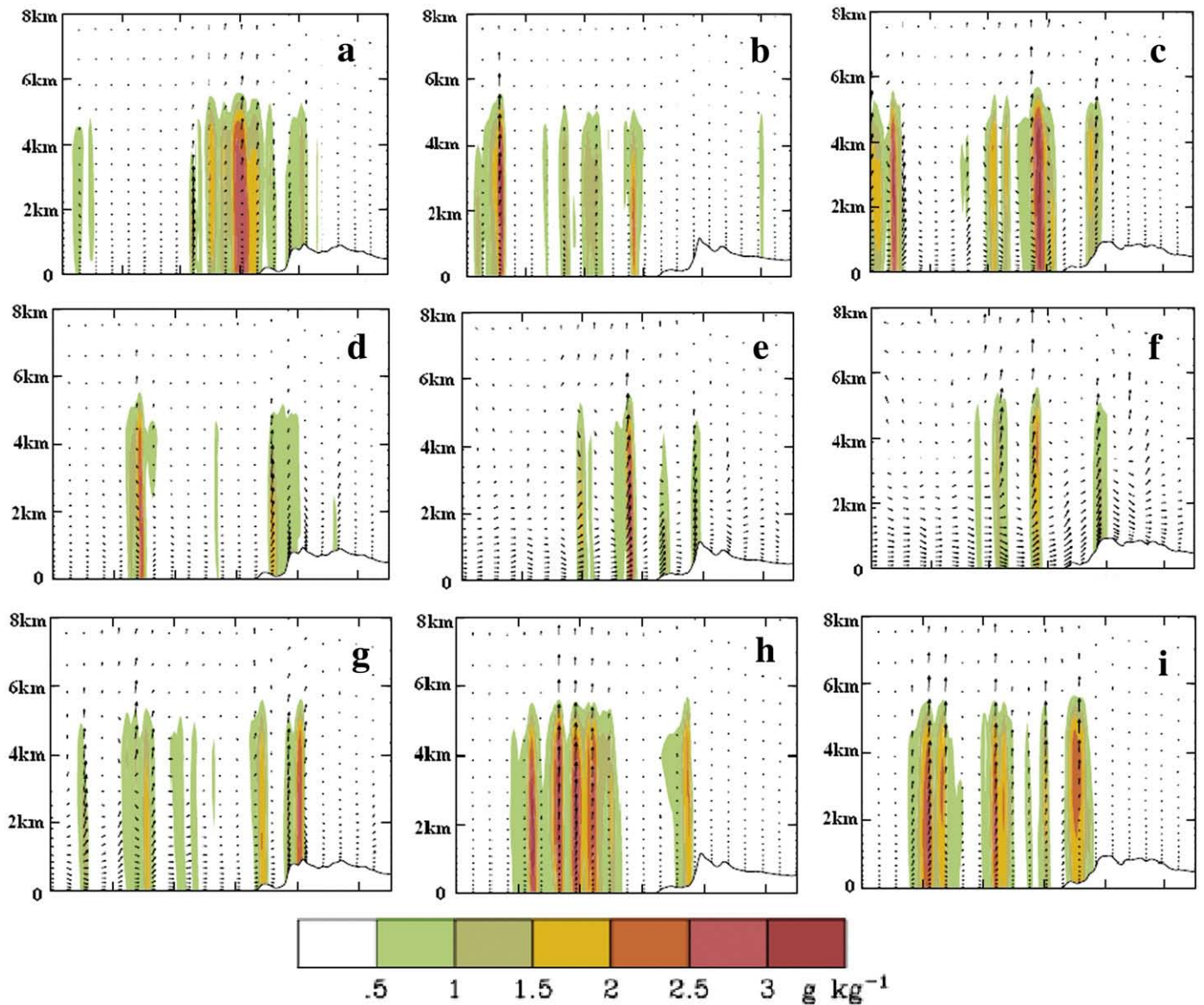


Fig. 15. Cross section plot at 19.11° latitude, 70°E–75°E longitude for rain water mixing ratio (g kg^{-1}) and circulation vectors for Noah control (first column), Noah-GEM (second column), and Slab (third column) runs at 00Z, July 26th (first row), 12Z, July 26th (second row), and 00Z, July 27th, 2005 (third row).

zone situated south and west of Mumbai. The Noah-GEM run resulted in an inland coastal divergence zone over Mumbai between two convergence zones—one offshore and other more inland. By 12Z, the convergence/divergence couplet is apparent only in the 500 mb level while the 850 mb fields show a stronger convergence zone over Mumbai. The 500 mb couplet weakened, but persisted for the next 12 h. The most notable intense surface convergence pattern was seen in the Slab run. A convergence zone was produced in and around Mumbai with divergence in southern India (near Bangalore); at 12Z, July 26th, the convergence zone gained strength and moved inland at both the 850 mb and 500 mb levels. Over the next 12 h, the convergence zone moved southward at the 850 mb level in the Slab model, whereas throughout the simulation time period, the 500 mb level indicated a convergence/divergence pattern south of Mumbai from the Slab model. The 100 mb plots show a divergence zone intensifying over Mumbai for all three runs by 00Z, July 27th, and the divergence zone is accompanied by a weak zone of convergence along the Indian west coast.

The convergence/divergence patterns are significant as they provide the mechanism for moisture transfer that can result in model rainfall. A cross-section taken over Mumbai (19.11°N, 70°E–

75°E) for a region spanning 100 km inland and offshore provided additional evidence of significant differences between the three cases. The simulated rain water mixing ratio fields for the three runs are shown in Fig. 15. The cross section suggests a cloud depth of approx. 6 km, which is comparable, but lower than, the 8 km deep cloud depth estimated in the observations reported by Shyamala and Bhadram (2006). The Slab model run had the highest rain water mixing ratio as compared to the Noah and Noah-GEM runs (Fig. 15). The Slab run also simulated several individual rain cells with a persistent westerly wind near the coast and over the ocean. The constant moisture supply at the surface, and the high cloud water mixing ratio in the vertical atmosphere, could have created the right conditions for the heavy Mumbai rainfall. Stronger near surface winds showed in the Noah control run at 00Z, July 26th, as the strong upward motion moved westward with time. The location of strong vertical winds simulated by the Noah-GEM show a lower cloud water mixing ratio, as compared to the Noah.

Fig. 16 shows the column integrated perceptible water (CIPW) content for the three model runs. Consistent with the convergence/divergence plots, the Noah and Noah-GEM produced cloud bands and

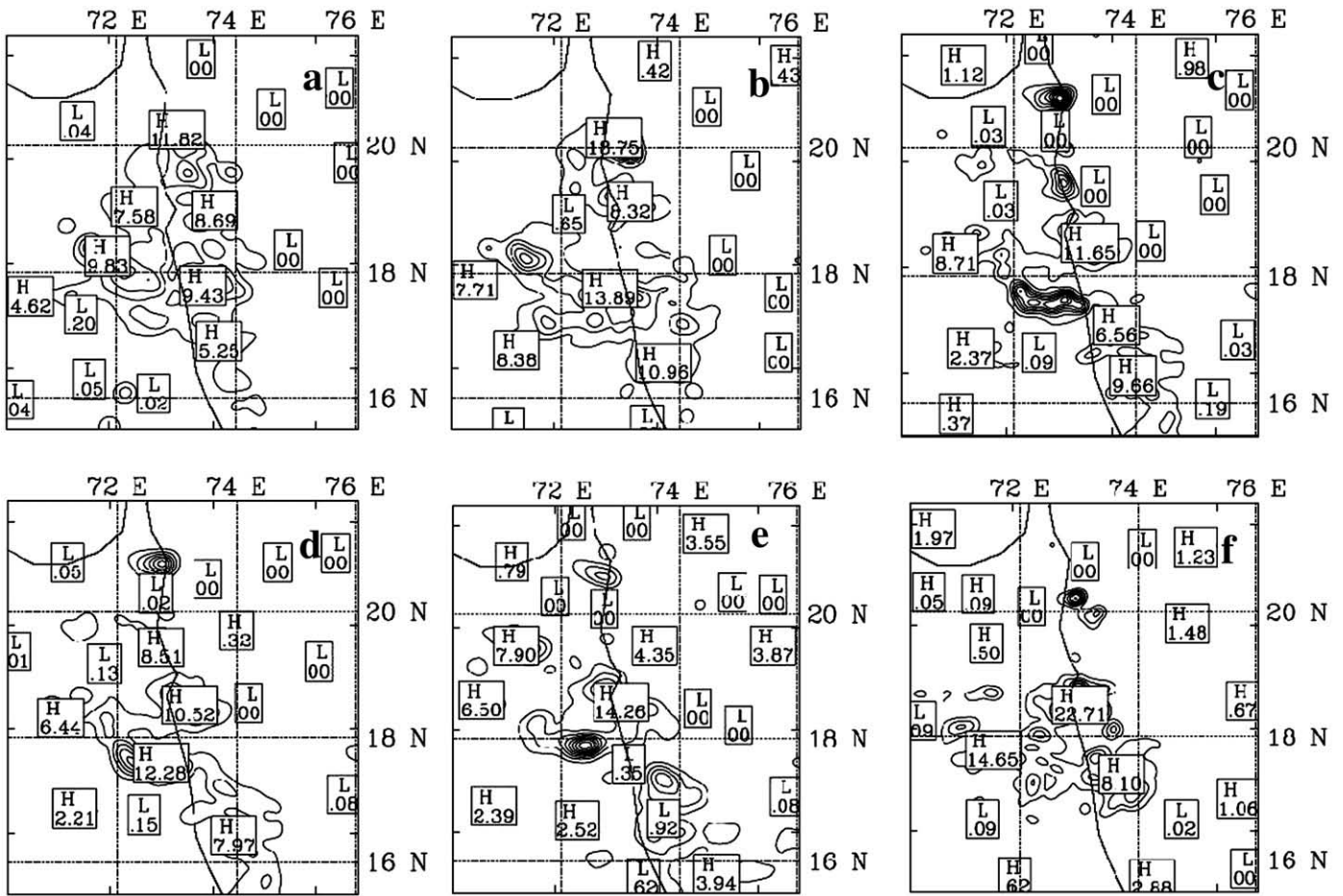


Fig. 16. Column integrated perceptible water (CIPW) for Noah (first column), Noah-GEM (second column) and Slab (third column) at 06Z (first row) and 18Z, July 26th (second row).

higher values of CIPW over the Western Ghats, while Slab produced a cloud water band south of Mumbai. Interestingly, each of the three model runs shows a hotspot over Mumbai, which clearly seen in the Slab run at 18Z, July 26th. Also, all three runs resulted in different CIPW both in terms of amounts and distribution. Therefore, the three LSMs are expected to create different rainfall values over Mumbai and the vicinity, as discussed in the following section.

4.5. Rainfall analysis

The WRF control run was able to reproduce the 24-h heavy rain over western India with maximum rainfall over Mumbai (Fig. 17). Both the Noah and Noah-GEM simulated three rainfall hotspots along the

Western Ghats, while Slab simulated two larger intense rainfall locations with a higher precipitation amounts. All three LSM runs missed the concurrent widespread inland rains over central India. Also, the Slab produced a rain band extending into the Arabian Sea, which was neither seen in the observation, nor in the Noah and Noah-GEM runs. Although the simulated rainfall amount did not match the observed value, it should be noted that these simulated maximum rainfall values are significantly larger (and closer to observation) than those obtained in previous studies for this case.

The model simulated the rainfall time series for six locations (as shown in Fig. 18): Colaba (18.93°N, 72.85°E), Santa Cruz (19.2°N, 72.53°E), Vihar Lake (19.14°N, 72.53°E), Pen (18.73°N, 73.09°E), Poinad (18.62°N, 73.11°E) and Wagbil (19.25°N, 72.97°E). These stations are

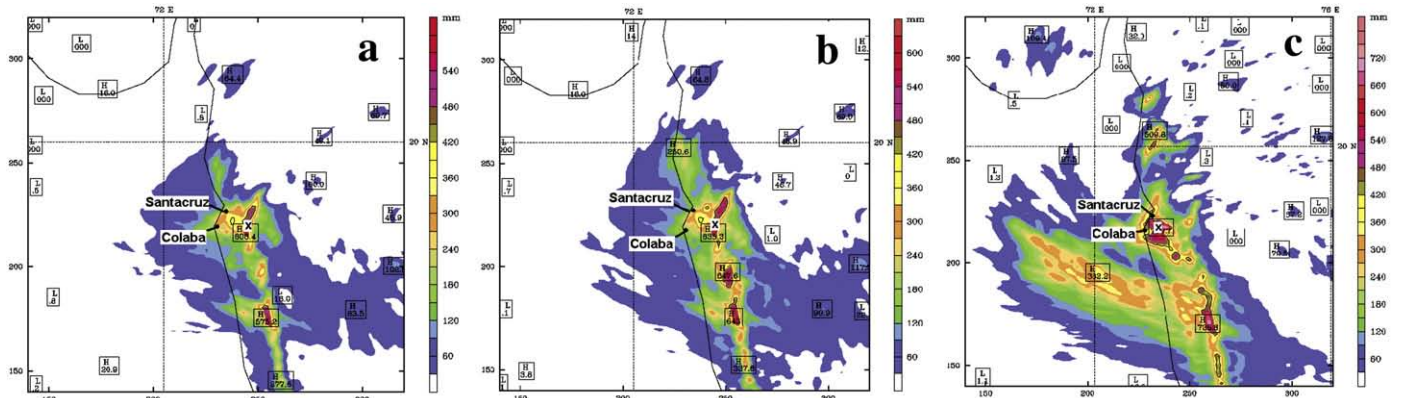


Fig. 17. Simulated 24-h rain amount and pattern (from 00Z, July 26th to 00Z, July 27th) in 3.3 km resolution from (a) Noah control, (b) Noah-GEM, and (c) Slab.

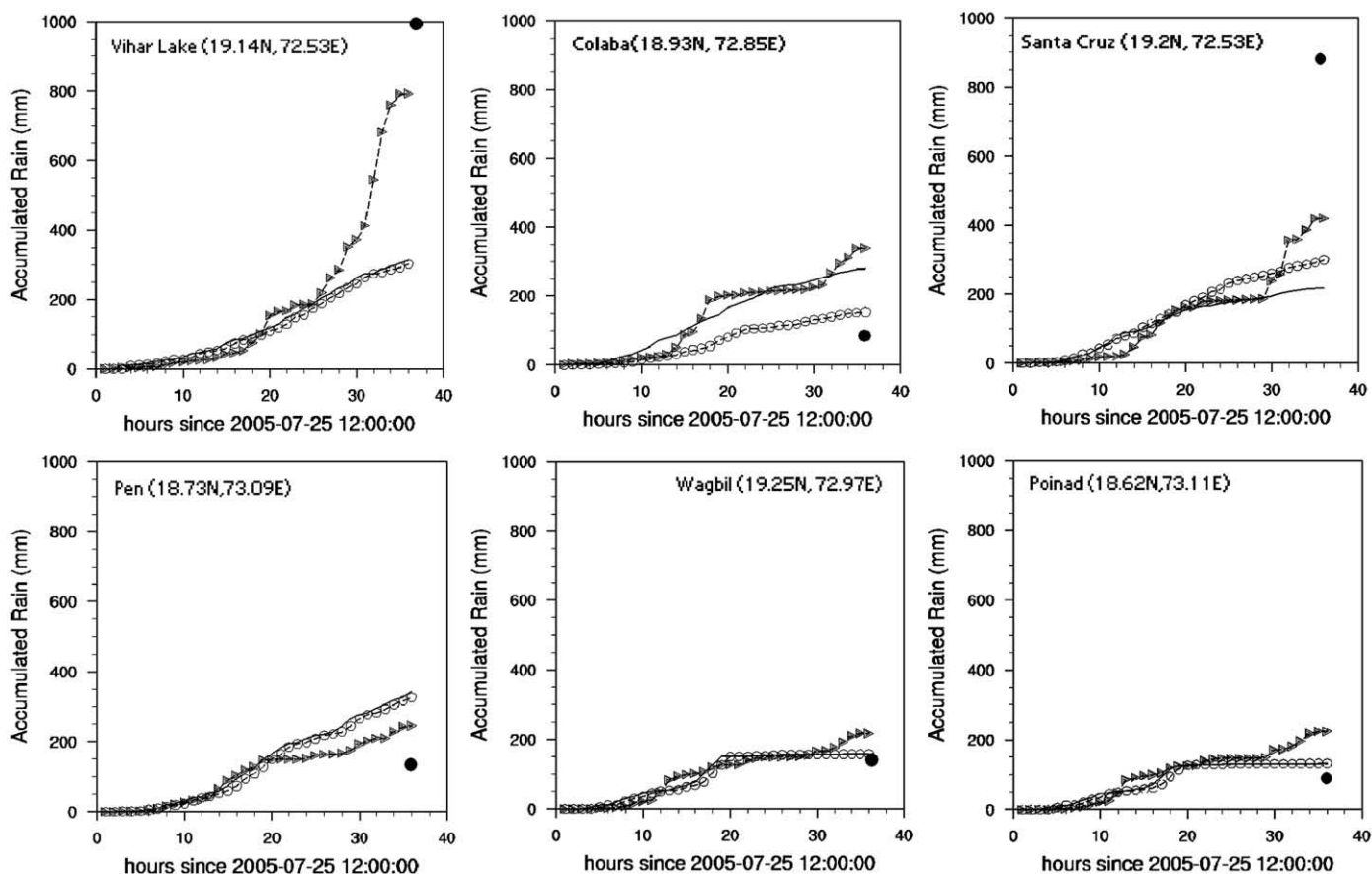


Fig. 18. Rainfall time series from LSM sensitivity runs for selected stations. Time series starts at 00Z, July 25th, and observed accumulated rainfall amount is shown at 00Z, July 27th. Closed circles are observed total rainfall (mm), solid line represents Noah control run, dashed line with closed triangle shows Slab model run, and dashed line with open circle depicts Noah-GEM run.

located within about 100 km around the Mumbai area, and are selected based on availability of observations. Recall that the observed rainfall totals of this event showed large spatial variability for Santa Cruz and Colaba measuring at 944 mm and 74 mm, respectively. Of the three runs, the Slab run simulated the highest rainfall between Santa Cruz (450 mm) and Colaba (380 mm). The Noah-GEM simulated approximately 300 mm for Santa Cruz and about 150 mm for Colaba, while the Noah control run simulated 200 mm for Santa Cruz and 300 mm for Colaba. The observed highest rainfall for this heavy rain event occurred near Vihar Lake (northeast of the Santa Cruz airport) with 24-h rainfall totals in excess of 1040 mm. The Noah and Noah-

GEM runs only simulated about 300 mm, however, and the Slab run simulated about 800 mm accumulated precipitation from 00Z, July 26th to 00Z, July 27th. The rainfall time series for Colaba, Pen, Poinad, and Wagbil indicated that all three LSM runs overestimated the precipitation amount, while the model runs underestimated the total rainfall in Vihar Lake and Santa Cruz. The highest rainfall totals for the three runs were: 781 mm in the Slab; 733 mm in the Noah control, and 678 mm in the Noah-GEM runs. The maximum rainfall location in the Slab model run (18.9°N, 72.9°E) was about 50 km west and 30 km north of the location simulated by the Noah (18.6°, 73.5°E) and the Noah-GEM (18.7°, 73.4°E) runs. Compared with the maximum rainfall

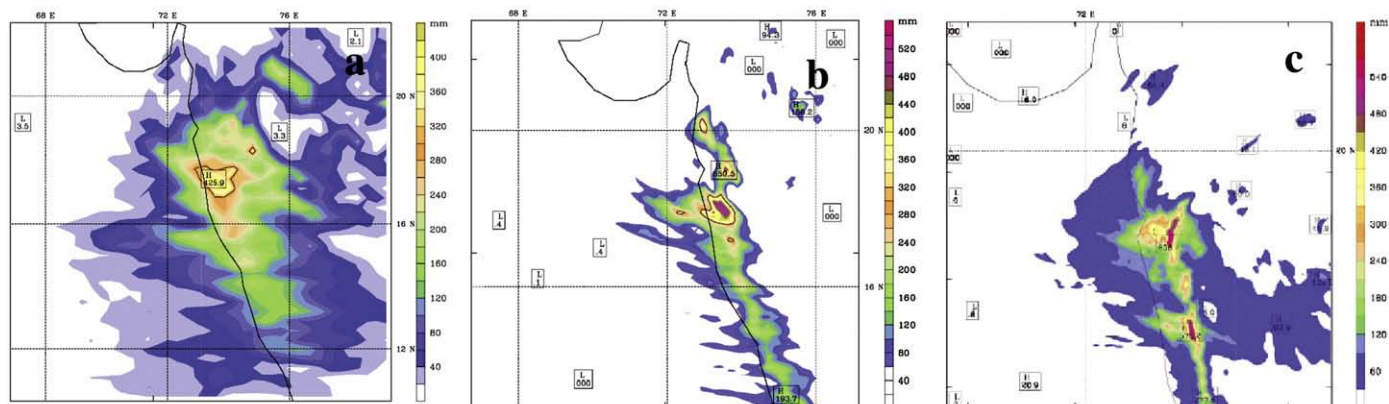


Fig. 19. Simulated rainfall from Noah control run shown in 3.3 km resolution domain size from (a) 30 km resolution output (b) 10 km resolution output, and (c) 3.3 km resolution output. The 30 km resolution run uses Grell-Devenyi cumulus parameterization scheme, when 10 km and 3.3 km resolution runs have explicit convection.

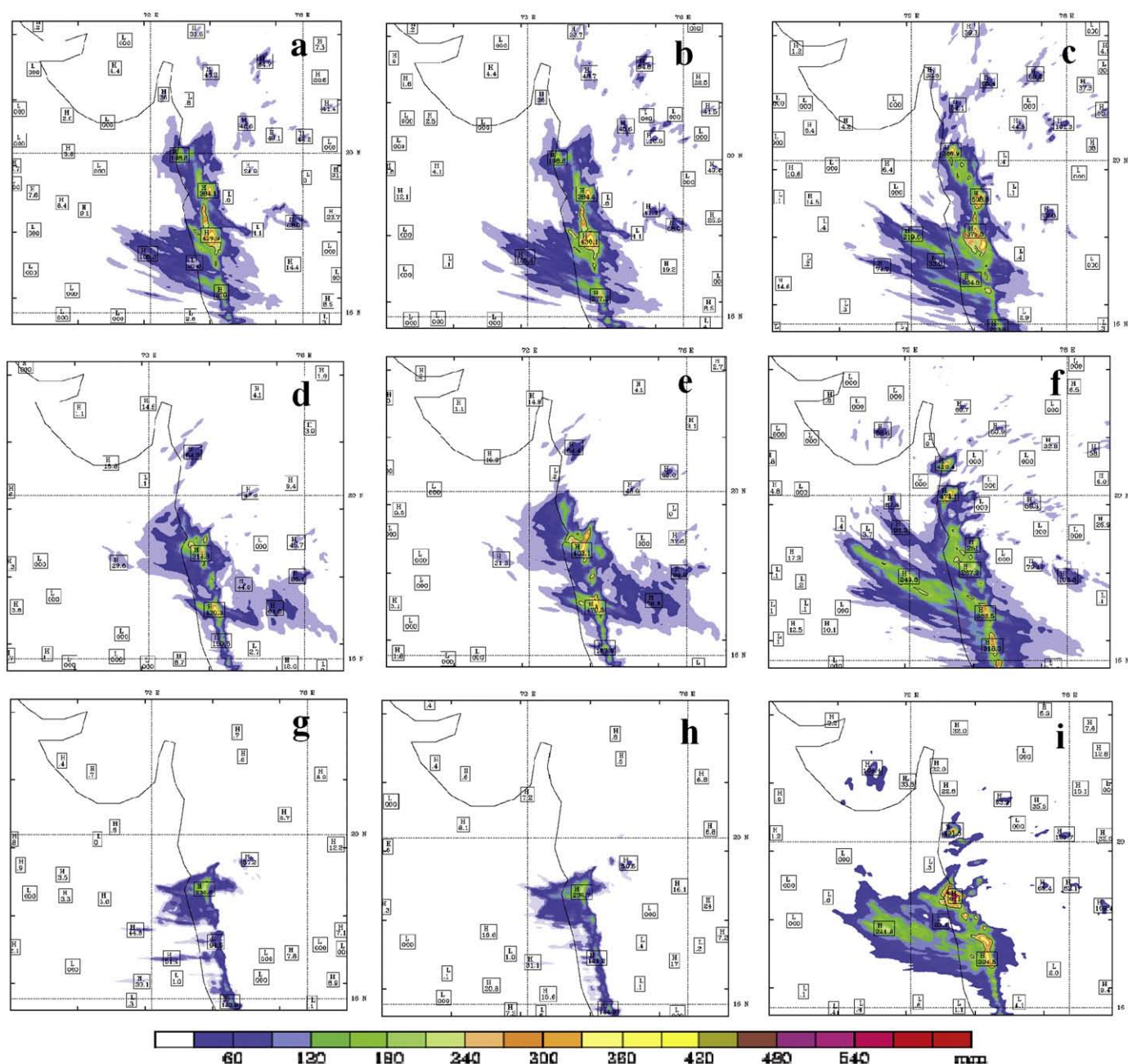


Fig. 20. 12-h accumulated rainfall in the 3.3 km resolution domain from Noah control (first column), Noah-GEM (second column), and Slab (third column) for 12Z, July 25th to 00Z, July 26th (first row), 00Z to 12Z, July 26th (second row), and 12Z, July 26th to 00Z, July 27th (third row).

location (Mumbai, 19.2°N, 72.53°E), results from all three LSM runs simulated the heaviest rain closer to Colaba (18.93°N, 72.85°E) as compared to Santa Cruz (as seen in the observations).

In order to bring the model results into perspective with prior model case studies, the effect of grid spacing was examined. Fig. 19 shows the rainfall distribution for the innermost domain with the 30 km, 10 km, and 3.3 km resolution run. Interestingly, all three domains indicated heavy rain near Mumbai city, though the amounts and distribution varied. The rainfall intensity increased with finer model resolution. Fig. 20 shows the 12-h accumulated precipitations. The Noah-GEM-simulated precipitation region is relatively similar to the Noah control simulation. For the 12-h duration starting 12Z, July 25th, the Noah and Noah-GEM runs (Fig. 20a and b) simulated similar rain distributions with two rain cells having the highest precipitation at approximately 430 mm further south of Mumbai, and a connecting rain band along the Western Ghats. The Slab run simulated three rain cells (Fig. 20c) with the

highest rainfall in excess of 500 mm for the 12 h period. Between 00Z and 12Z on July 26th, the rain band along Western Ghats has slightly weakened (Fig. 20f), while the two cells in the Noah and the Noah-GEM still produce high amount of precipitation (more than 400 mm over 12 h in Fig. 20d and e). At approximately 12Z, July 26th and 00Z, July 27th, the heavy rain in the Noah and the Noah-GEM (Fig. 20g and h) has dissipated; while the Slab run shows reintensified convection resulting in heavy rain in the region of Mumbai city (Fig. 20i). Thus, the WRF model response for the three LSMs indicates significant differences in the simulation of rainfall timing, distribution, and amount.

5. Discussions and conclusions

This study investigated the impact of land surface processes on the performance of a mesoscale model—the Weather Research Forecasting (WRF) model (WRF-ARW)—for the simulation of the July 26th, 2005

heavy rain event over Mumbai. A related objective was to evaluate the ability of the WRF model to simulate the extreme Mumbai rain event. Overall, the WRF model reasonably reproduced the localized heavy rain event over Mumbai, and the higher resolution domain (3.3 km grid spacing) showed better model performance (as compared to the 10 km and 30 km resolution domains). The results also suggest that the model response was significantly different in terms of surface fluxes, boundary layer parameterization, and resulting wind circulations and dynamical patterns for different land surface models. The rainfall timing, location, intensity, and precipitation amounts were sensitive to the land surface representations within the WRF model.

To further demonstrate the impact of land surface feedback, we conducted additional synthetic experiments, including the study of replacing the crops landuse with forest (to represent the potential natural landscape). Model results were compared with a control (current land use) simulation, as well as with experiments involving various domain resolutions. The land use/land cover sensitivity tests showed that land surface feedback could result in broader areal and dynamical impacts on rainfall intensity and distribution. The coupled WRF model results were sensitive to land use land cover change even for this intense heavy rain event. We also conducted experiments with two different start times in order to compare the impact of boundary conditions. Simulations were made with start time that was 6 h earlier (06Z, July 25th) and 6 h later (18Z, July 26th) than the WRF control run. The resulting impact on precipitation simulation was relatively moderate (figure not shown). The accumulated 24 h rainfall from the rain cell closest to Mumbai city appears to be the highest for the WRF control runs (606 mm), and about 50 mm to 120 mm higher than the 6 h earlier and the 6 h later runs, respectively. Comparing the results between the three LSM runs, we found that the impact of the LSM change, particularly the Slab versus the Noah, showed a more dramatic difference than the start time change experiments, which reaffirms our conclusions that while synoptic boundary conditions are critical to transporting the moisture to the region (cf. Vaidya and Kulkarni 2006), the mesoscale (the land surface) feedback is also important in affecting the time, location and intensity of the rainfall.

Building on the conclusions of Niyogi et al. (2006) and Holt et al. (2006), it was expected that a more detailed LSM (such as Noah-GEM) would result in an overall better-coupled model quantitative precipitation forecast (QPF). In our study, the Slab model was the simplest of the three LSMs, and the Noah-GEM was the most complex. The Noah and Noah-GEM simulated nearly similar rainfall performance and rainfall distribution with a modest difference in rainfall amounts. In contrast, the simplest Slab run simulated much stronger convective activity, better spatial convergence fields, resulted in the highest accumulated precipitation (that was closest to the observations). Indeed, while Slab simulated the highest rainfall amount over Mumbai, the rainfall distribution was more offshore as compared to satellite observations. Both Noah and Noah-GEM produced more wide spread inland rainfall, and also simulated rains south of Mumbai along the Western Ghats. Although all three WRF LSM experiments simulated relatively better results than other operational models, the results suggest high uncertainty in the ability of the WRF model to simulate this highly localized heavy rain event in terms of timing, location, and intensity. One reason for the lack of significant improvement in the model performance with Noah and Noah-GEM could have been the outdated land surface dataset in the model. Due to the inconsistency of the model performance, especially in the urban area, and the model sensitivity to land surface processes, additional studies are needed with updated land surface information, as well as explicit soil moisture and soil temperature data for the Indian monsoon region.

Based on the various numerical experiments and comparisons with available observations, we conclude that:

- (1) the WRF control simulation coupled with the Noah land surface model simulated the highly localized Mumbai rain event

moderately well in terms of rainfall amount and convection structure over Mumbai, as compared to other weather forecast model results for the Mumbai heavy rain event reported in the literature.

- (2) The various WRF runs suggest a good ability overall to simulate vertical temperature structure, and a modest to poor ability to simulate humidity and wind fields. Noah and Noah-GEM runs resulted in a deep circulation over Mumbai. The Slab run produced a well-defined convergence zone over Mumbai.
- (3) The selection of the Grell–Devenyi convective parameterization scheme resulted in a better overall model performance, as compared to the Betts–Miller–Janjic and Kain–Fritsch schemes. Consistent with prior studies, the model performance was better with a finer grid spacing (higher resolution) set up using the Grell–Devenyi parameterization scheme. More specifically, the 3.3 km grid spacing model performance was better than the 10 km, and this grid spacing was better than the model results for the 30 km model grid spacing (based on the accumulated rainfall simulations). Thus, the heavy rainfall forecasting would likely remain significantly uncertain with models that have coarser grid spacing (e.g. climate models), and with model configurations which have not been extensively tested over the Indian monsoon region.
- (4) Although the Slab, Noah, and Noah-GEM LSMs coupled to the WRF-ARW were able to produce relatively high maximum precipitation amounts (order of 700 mm) around Mumbai, significant differences in the model results were reported for the three schemes related to surface, boundary layer, and dynamical feedbacks, including rainfall amounts over locations such as Santa Cruz and Colaba. The results from the model experiments analyzed in this study provide additional evidences that land surface representation has a prominent feedback on the representation of mesoscale convection and heavy rain processes for heavy rain events over the Indian monsoon region. The changes in surface characteristics can affect the convection dynamics and precipitation patterns in terms of location, timing, and intensity of precipitation. The findings in this paper need to be verified with additional heavy rain case studies in the Indian monsoon region, and up-to-date land use land cover information is needed when evaluating the impact of land surface schemes.

An intriguing question has resulted from our findings which concerns the equal or even occasionally better performance of the simpler Slab model in comparison to the more sophisticated land surface models in the simulation of this heavy rain event over the Indian monsoon region. Further evaluation and possibly calibration of the variables used in the land surface schemes over the Indian Monsoon Region, in tandem with further customization involving different convection and physical parameterization schemes, are needed to assess these discrepancies in simulation accuracy.

Acknowledgements

The authors would like to acknowledge and NSF-ATM 0233780 (Dr. S. Nelson), NASA-THP (Dr. J. Entin NNG05GQ47G and NNG06GH17G), NASA-IDS (NNG04GL61G Drs. J. Entin and G. Gutman) and the NASA Land Use Land Cover Change Program (Dr. G. Gutman) and NCAR Water Cycle Across Scale program at The Institute for Integrative and Multidisciplinary Earth Studies and the NSF/NCAR USWRP program. The study also benefited from the Purdue Asian Initiative Program. We extend our thanks to the NASA Tropical Rainfall Measurement Mission (TRMM) for Fig. 1b, and to one of the reviewers for providing a clearer version of Fig. 1a used in this paper. We thank the four reviewers' constructive comments that resulted in this substantially enhanced manuscript.

References

- Azadi, M., Mohanty, U.C., Madan, O.P., Padmanabhamurty, B., 2002. Prediction of precipitation associated with a western disturbance using a high-resolution regional model: role of parameterisation of physical processes. *Meteorol. Appl.* 9, 317–326.
- Bohra, A.K., Basu, Swati, Rajagopal, E.N., Iyengar, G.R., Das Gupta, M., Ashrit, R., Athiyaman, B., 2006. Heavy rainfall episode over Mumbai on 26 July 2005: assessment of NWP guidance. *Curr. Sci.* 90, 1188–1194.
- Chang, H., Niyogi, D., Mohanty, U.C., Routray, A. and Gupte, M., 2005: Impacts of land use changes on heavy precipitation over the Indian monsoonal regions, AGU Fall Meeting, San Francisco, December 2005. <http://www.agu.org/cgi-bin/SFgate/SFgate?&listenv=table&multiple=1&range=1&directget=1&application=fm05&database=%2Fdata%2Fepubs%2Fwais%2Findexes%2Ffm05%2Ffm05&maxhits=200&=B41A-0168>.
- Chen, F., Dudhia, J., 2001. Coupling an advanced land surface–hydrology model with the Penn State-NCAR MM5 modeling system. Part I: model implementation and sensitivity. *Mon. Weather Rev.* 129, 569–585.
- Deardorff, J.W., 1978. Efficient prediction of ground surface temperature and moisture, with an inclusion of a layer of vegetation. *J. Geophys. Res.* 83, 1889–1903.
- Ek, M.B., Mitchell, K.E., Lin, Y., Rogers, E., Grunmann, P., Koren, V., Gayno, G., Tarpley, J.D., 2003. Implementation of Noah land surface model advances in the National Centers for Environmental Prediction operational mesoscale Eta model. *J. Geophys. Res.* 108, 8851. doi:10.1029/2002JD003296.
- Holt, T., Niyogi, D., Chen, F., LeMone, M.A., Manning, K., Qureshi, A.L., 2006. Effect of land–atmosphere interactions on the IHOP 24–25 May 2002 convection case. *Mon. Weather Rev.* 134, 113–133.
- Jenamani, R.K., Bhan, S.C., Kalsi, S.R., 2006. Observational/forecasting aspects of the meteorological event that caused a record highest rainfall in Mumbai. *Curr. Sci.* 90 (10), 1344–1363.
- Koren, V., Schaake, J., Mitchell, K., Duan, Q.Y., Chen, F., Baker, J.M., 1999. A parameterization of snowpack and frozen ground intended for NCEP weather and climate models. *J. Geophys. Res.* 104, 19569–19585.
- Koster, 2004. Regions of strong coupling between soil moisture and precipitation. *Science* 305, 1138–1141.
- NCDC, 2007. National Climatic Data Center. (accessed 10 March 2007). <http://www.ncdc.noaa.gov/oa/climate/research/2005/jul/hazards.html>.
- Niyogi, D., 2000: Biosphere–atmosphere interactions coupled with carbon dioxide and soil moisture changes. Ph. D. Dissertation NC State Univ. Available from www.lib.ncsu.edu.
- Niyogi, D., Holt, T., Zhong, S., Pyle, P.C., Basara, J., 2006. Urban and land surface effects on the 30 July 2003 MCS event observed in the southern great plains. *J. Geophys. Res.* 111, D19107. doi:10.1029/2005JD006746.
- Noilhan, J., Planton, S., 1989. A simple parameterization of land surface processes for meteorological models. *Mon. Weather Rev.* 117, 536–549.
- Shyamala, B., Bhadrani, C.V.V., 2006. Impact of mesoscale–synoptic scale interactions on the Mumbai historical rain event during 26–27 July 2005. *Curr. Sci.* 91, 1649–1654.
- Trier, S., Chen, F., Manning, K., 2004. A study of convection initiation in a mesoscale model using high-resolution land surface initiation conditions. *Mon. Weather Rev.* 132, 2954–2976.
- Vaidya, S.S., 2006. The performance of two convective parameterization schemes in a mesoscale model over the Indian region. *Meteorol. Atmos. Phys.* 92, 175–190.
- Vaidya, S.S., Kulkarni, J.R., 2006. Simulation of heavy precipitation over Santacruz, Mumbai on 26 July 2005, using a mesoscale model. *Meteorol. Atmos. Phys.* doi:10.1007/s00703-006-0233-4.
- Venkata Ratnam, J., Cox, E.A., 2006. Simulation of monsoon depressions using MM5: sensitivity to cumulus parameterization schemes. *Meteorol. Atmos. Phys.* 93, 53–78.
- Xavier, V.F., Chandrasekar, A., Singh, R., Simon, B., 2006. The impact of assimilation of MODIS data for the prediction of a tropical low-pressure system over India using a mesoscale model. *Int. J. Remote Sens.* 27, 4655–4676.
- Yasunari, T., Saito, K., Takata, K., 2006. Relative roles of large-scale orography and land surface processes in the global hydroclimate. Part I: impacts on monsoon systems and the tropics. *J. Hydrometeorol.* 7, 626–641.